arXiv:cond-mat/0611163v1 [cond-mat.soft] 6 Nov 2006

# Current rectification, switching, polarons, and defects in molecular electronic devices

A.M. Bratkovsky

Hewlett-Packard Laboratories, 1501 Page Mill Road, Palo Alto, California 94304

Devices for nano- and molecular size electronics are currently a focus of research aimed at an efficient current rectification and switching.[1] A few generic molecular scale devices are reviewed here on the basis of first-principles and model approaches. Current rectification by (ballistic) molecular quantum dots can produce the rectification ratio $\leq 100$. Current switching due to conformational changes in the molecules is slow, on the order of a few kHz. Fast switching ($\sim$1 THz) may be achieved, at least in principle, in a degenerate molecular quantum dot with strong coupling of electrons with vibrational excitations. We show that the mean-field approach fails to properly describe *intrinsic* molecular switching and present an exact solution to the problem. Defects in molecular films result in spurious peaks in conductance, apparent negative differential resistance, and may also lead to unusual temperature and bias dependence of current. The observed switching in many cases is *extrinsic*, caused by changes in molecule-electrode geometry, molecule reconfiguration, metallic filament formation through, and/or changing amount of disorder in a molecular film. We give experimental examples of telegraph "switching" and "hot spot" formation in the molecular films.

## 1 Introduction

Current interest in molecular electronics is largely driven by expectations that molecules can be used as nanoelectronics components able to complement/replace standard silicon CMOS technology[1, 2] on the way down to $\leq$10nm circuit components. The first speculations about molecular electronic devices (diodes, rectifiers) were apparently made in mid-1970s[3]. That original suggestion of a molecular rectifier has generated a large interest in the field

[1] Chapter from: *Polarons in Advanced Materials*, edited by A. S. Alexandrov (Canopus/Springer, Bristol, 2007).

and a flurry of suggestions of various molecular electronics components, especially coupled with premature estimates that silicon-based technology cannot scale to below $1\mu$m feature size. The Aviram-Ratner's Donor-insulator-Acceptor construct TTF$-\sigma-$TCNQ ($D^+ - \sigma - A^-$, see details below), where carriers were supposed to tunnel asymmetrically in two directions through insulating saturated molecular $\sigma-$'bridge', has never materialized, in spite of extensive experimental effort over a few decades [4]. End result in some cases appears to be a slightly electrically anisotropic *insulator,* rather than a diode, unsuitable as a replacement for silicon devices. This comes about because in order to assemble a reasonable quality monolayer of these molecules in Langmuir-Blodgett trough (avoiding defects that will short the device after electrode deposition) one needs to attach a long 'tail' molecule C18 [$\equiv (CH_2)_{18}$] that can produce enough of a Van-der-Waals force to keep molecules together, but C18 is a wide-band insulator with a bandgap $E_g \approx 9 - 10$eV. The outcome of these studies may have been anticipated, but if one were able to assemble the Aviram-Ratner molecules without the tail, they could not rectify anyway. Indeed, a recent ab-initio study[5] of $D^+\sigma A^-$ prospective molecule showed no appreciable asymmetry of its I-V curve. The molecule was envisaged by Ellenbogen and Love[6] as a 4-phenyl ring Tour wire with dimethylene insulating bridge in the middle directly connected to Au electrodes via thiol groups. Donor-acceptor asymmetry was produced by side $NH_2^+$ and $NO_2^-$ moieties, which is a frequent motif in molecular devices using the Tour wires. The reason of poor rectification is simple: the bridge is too short, it is a transparent piece of one-dimensional insulator, whereas the applied field is three dimensional and it cannot be screened efficiently with an appreciable voltage drop on the insulating group in this geometry. Although there is only 0.7eV energy separation between levels on the D and A groups, one needs about 4eV bias to align them and get a relatively small current because total resonant transparency is practically impossible to achieve. Remember, that the model calculation implied an ideal coupling to electrodes, which is impossible in reality and which is known to dramatically change the current through the molecule (see below). We shall discuss below some possible alternatives to this approach.

It is worth noting that studies of energy and electron transport in molecular crystals [7] started already in early 1960s. It was established in mid-1960s in what circumstances charge transport in biological molecules involves electron tunneling [8]. It was realized in mid-1970s that since the organic molecules are 'soft', energy transport along linear biological molecules, proteins, etc. may proceed by low energy nonlinear collective excitations, like Davydov solitons [9] (see review [10]).

To take over from current silicon CMOS technology, the molecular electronics should provide smaller, more reliable, functional components that can be produced and assembled concurrently and are compatible with CMOS for integration. The small size of units that molecules may hopefully provide is quite obvious. However, meeting other requirements seems to be a

very long shot. To beat alternative technologies for e.g. dense (and cheap) memories, one should aim at a few Tb/in$^2$ ($> 10^{12} - 10^{13}$ bit/cm$^2$), which corresponds to linear bit (footprint) sizes of $3 - 10$ nanometers, and an operation lifetime of $\sim 10$ years. The latter requirement is very difficult to meet with organic molecules that tend to oxidize and decompose, especially under conditions of very high applied electric field (given the operational voltage bias of $\sim$ 1V for molecules integrated with CMOS and their small sizes on the order of a few nanometers). In terms of areal density, one should compare this with rapidly developing technologies like ferroelectric random access (FERAM)[11] or phase-change memories (PCM)[12]. The current smallest commercial nano-ferroelectrics are about $400\times400$ nm$^2$ and 20-150 nm thick [13], and the $128 \times 128$ arrays of switching ferroelectric pixels bits have been already demonstrated with a bit size $\leq$ 50nm (with density $\sim$Tb/in$^2$)[14]. The phase-change memories based on chalcolgenides GeSbTe (GST) seem to scale even better than the ferroelectrics. As we see, the mainstream technology for random-access memory approaches molecular size very rapidly. At the same time, the so-called "nanopore" molecular devices[35] have comparable sizes and yet to demonstrate a repeatable behavior (for reasons explained below).

In terms of parallel fabrication of molecular devices, one is looking at *self-assembly* techniques (see, e.g. [15, 16], and references therein). Frequently, the Langmuir-Blodgett technique is used for self-assembly of molecules on water, where molecules are prepared to have hydrophilic "head" and hydrophobic "tail" to make the assembly possible, see e.g. Refs. [17, 18]. The allowances for a corresponding assembly, especially of hybrid structures (molecules integrated on silicon CMOS), are on the order of a *fraction* of an Angstrom, so actually a *picotechnology* is required [2]. Since it is problematic to reach such a precision any time soon, the all-in-one molecule approach was advocated, meaning that a fully functional computing unit should be synthesized as a single supermolecular unit[2]. The hope is that perhaps directed self-assembly will help to accomplish building such a unit, but self-assembly on a large scale is impossible without defects[15, 16], since the entropic factors work against it. Above some small defect concentration ("percolation") threshold the mapping of even a simple algorithm on such a self-assembled network becomes impossible[19].

There is also a big question about electron transport in such a device consisting of large organic molecules. Even in high-quality pentacene (P5) crystals, perhaps the best materials for thin film transistors, the mobility is a mere 1-2 cm$^2$/V·s (see e.g. [20]), as a result of carrier trapping by interaction with a lattice and necessity to hop between P5 molecules. The situation with carrier transport through long molecules ($> 2 - 3$nm) is, of course, substantially different from the transport through short rigid molecules that have been envisaged as possible electronics components. Indeed, in *short* molecules the dominant mode of electron transport would be resonant tunneling through *electrically active* molecular orbital(s) [21], which, depending on the workfunction of the electrode, affinity of the molecule, and symmetry of coupling between

molecule and electrode may be one of the lowest unoccupied molecular orbitals (LUMO) or highest occupied molecular orbitals (HOMO)[22, 23]. Indeed, it is well known that in longer wires containing more than about 30-40 atomic sites, the tunneling time is comparable to or larger than the characteristic phonon times, so that the polaron (and/or bipolaron) can be formed inside the molecular wire [24]. There is a wide range of molecular bulk conductors with (bi)polaronic carriers. The formation of polarons (and charged solitons) in polyacetylene (PA) was discussed a long time ago theoretically in Refs. [25] and formation of bipolarons (bound states of two polarons) in Ref.[26]. Polarons in PA were detected optically in Ref.[27] and since then studied in great detail. There is an exceeding amount of evidence of the polaron and bipolaron formation in conjugated polymers such as polyphenylene, polypyrrole, polythiophene, polyphenylene sulfide [28], Cs-doped biphenyl [29], n-doped bithiophene [30], polyphenylenevinylene(PPV)-based light emitting diodes [31], and other molecular systems. Both intrinsic and extrinsic parameters play a role in determining the electrical and optical properties of polymer films: spatial range of $\pi$-electron delocalization, interchain interaction, morphology, amount of defects and disorder, carrier density, etc (for a brief review of carrier transport mechanisms and materials see Ref. [32]).

The latest wave of interest in molecular electronics is mostly related to recent studies of carrier transport in synthesized linear conjugated molecular wires (Tour wires[1]) with apparent non-linear I-V characteristics [negative differential resistance (NDR)] and "memory" effects[33, 34, 35], various molecules with a mobile *microcycle* that is able to move back and forth between metastable conformations in solution (molecular shuttles) [36] and demonstrate some sort of "switching" between relatively stable resistive states when sandwiched between electrodes in a solid state device[37] (see also [38]). There are also various photochromic molecules that may change conformation ("switch") upon absorption of light [39], which may be of interest to some photonics applications but not for the general purpose electronics. One of the most serious problems with using this kind of molecules is *power dissipation*. Indeed, the studied organic molecules are, as a rule, very resistive (in the range of $\sim 1\mathrm{M}\Omega - 1\mathrm{G}\Omega$, or more). Since usually the switching bias exceeds 0.5V the dissipated power density would be in excess of 10 kW/cm$^2$, which is orders of magnitude higher than the presently manageable level. One can drop the density of switching devices, but this would undermine a main advantage of using molecular size elements. This is a common problem that CMOS faces too, but organic molecules do not seem to offer a tangible advantage yet. There are other outstanding problems, like understanding an actual switching mechanism, which seems to be rather molecule-independent[38], stability, scaling, etc. It is not likely, therefore, that molecules will displace silicon technology, or become a large part of a hybrid technology in a foreseeable future.

First major moletronic applications would most likely come in the area of chemical and biological sensors. One of the current solutions in this area is to use the functionalized nanowires. When a target analyte molecule attaches

from the environment to such a nanowire, it changes the electrostatic potential "seen" by the carriers in the nanowire. Since the conductance of the nanowire device is small, even one chemisorbed molecule could make a detectable change of a conductance[40]. Semiconducting nanowires can be grown from seed metal nanoparticles[15], or it can be carbon nanotubes (CNT), which are studied extensively due to their relatively simple structure and some unique properties like very high conductance[41].

In this paper we shall address various generic problems related to electron transport through molecular devices, and describe some specific molecular systems that may be interesting for applications as rectifiers and switches, and some pertaining physical problems. We shall first consider systems where an elastic tunneling is dominant, and interaction with vibrational excitations on the molecules only renormalizes some parameters describing tunneling. We shall also describe a situation where the coupling of carriers to molecular vibrons is strong. In this case the tunneling is substantially inelastic and, moreover, it may result in current hysteresis when the electron-vibron interaction is so strong that it overcomes Coulomb repulsion of carriers on a central narrow-band/conjugated unit of the molecule separated from electrodes by wide band gap saturated molecular groups like $(CH_2)_n$, which we shall call a molecular quantum dot (molQD). Another very important problem is to understand the nature and the role of imperfections in organic thin films. It is addressed in the last section of the paper.

## 2 Role of molecule-electrode contact: extrinsic molecular switching due to molecule tilting

We have predicted some while ago that there should be a strong dependence of the current through conjugated molecules (like the Tour wires [1]) on the geometry of molecule-electrode contact [22, 23]. The apparent "telegraph" switching observed in STM single-molecule probes of the three-ring Tour molecules, inserted into a SAM of non-conducting shorter alkanes, has been attributed to this effect [34]. The theory predicts very strong dependence of the current through the molecule on the tilting angle between a backbone of a molecule and a normal to the electrode surface. Other explanations, like rotation of the middle ring, charging of the molecule, or effects of the moieties on the middle ring, do not hold. In particular, switching of the molecules *without* any $NO_2$ or $NH_2$ moieties have been practically the same as with them.

The simple argument in favor of the "tilting" mechanism of the conductance lies in a large anisotropy of the molecule-electrode coupling through $\pi$-conjugated molecular orbitals (MOs). In general, we expect the overlap and the full conductance to be maximal when the lobes of the $p$-orbital of the end atom at the molecule are oriented perpendicular to the surface, and smaller otherwise, as dictated by the symmetry. The overlap integrals of a $p$-orbital

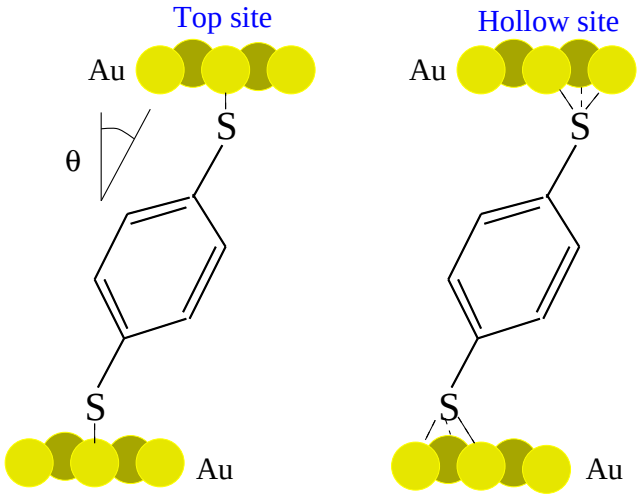


**Fig. 1.** Schematic representation of the benzene-dithiolate molecule on top and hollow sites. End sulfur atoms are bonded to one and three surface gold atoms, respectively, $\theta$ is the tilting angle.

with orbitals of other types differ by a factor about 3 to 4 for the two orientations. Since the conductance is proportional to the square of the matrix element, which contains a product of two metal-molecule hopping integrals, the total conductance variation with overall geometry may therefore reach two orders of magnitude, and in special cases be even larger.

In order to illustrate the geometric effect on current we have considered a simple two-site model with $p-$orbitals on both sites, coupled to electrodes with $s-$orbitals [23]. For non-zero bias the transmission probability has the resonant form (5) with line widths for hopping to the left (right) lead $\Gamma_L$ ($\Gamma_R$) . The current has the approximate form (with $\Gamma = \Gamma_L + \Gamma_R$)

$$I \approx \begin{cases} \frac{q^2}{h}\frac{\Gamma^2}{t^2}V \propto \sin^4\theta, & qV \ll E_{\rm LUMO} - E_{\rm HOMO}, \\ \frac{8\pi q}{h}\frac{\Gamma_L\Gamma_R}{\Gamma_L+\Gamma_R} \propto \sin^2\theta, & qV > E_{\rm LUMO} - E_{\rm HOMO}, \end{cases} \tag{1}$$

where $\theta$ is the tilting angle[23, 22], Fig. 1.

The tilting angle has a large effect on the I-V curves of benzene-dithiolate (BDT) molecules, especially when the molecule is anchored to the Au electrode in the top position, Fig. 2. By changing $\theta$ from 5° to just 15°, one drives the I-V characteristic from the one with a gap of about 2V to the ohmic one with a large relative change of conductance. Even changing $\theta$ from 10° to 15° changes the conductance by about an order of magnitude. The I-V curve for the hollow site remains ohmic for tilting angles up to 75° with moderate changes of conductance. Therefore, if the molecule in measurements snaps from the top to the hollow position and back, it will lead to an apparent

switching [34]. It has recently been realized that the geometry of a contact strongly affects coherent spin transfer between molecularly bridged quantum dots [42]. It is worth noting that another frequently observed *extrinsic* mechanism of "switching" in organic layers is due to electrode material diffusing into the layer and forming metallic "filaments" (see below).

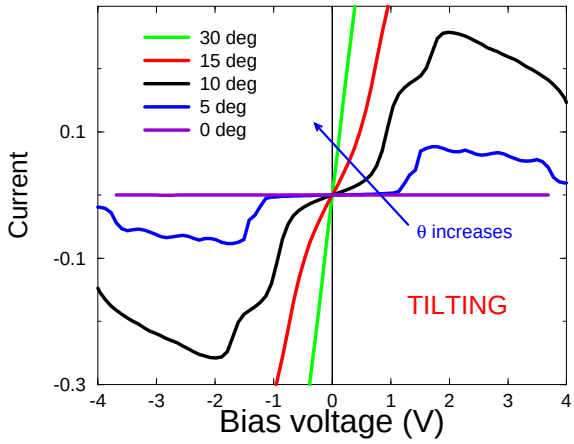


**Fig. 2.** Effect of tilting on I-V curve of the BDT molecule, Fig. 1. Current is in units of $I_0 = 77.5\mu$A, $\theta$ is the tilting angle.

## 3 Molecular quantum dot rectifiers

Aviram and Ratner speculated about a rectifying molecule containing donor ($D$) and acceptor ($A$) groups separated by a saturated $\sigma$-bridge (insulator) group, where the (inelastic) electron transfer will be more favorable from $A$ to $D$ [3]. The molecular rectifiers actually synthesized, $C_{16}H_{33} - \gamma$Q3CNQ, were of somewhat different $D - \pi - A$ type, i.e. the "bridge" group was conjugated [4]. Although the molecule did show rectification (with considerable hysteresis), it performed rather like an anisotropic insulator with tiny currents on the order of $10^{-17}$A/molecule, because of the large alkane "tail" needed for LB assembly. It was recently realized that in this molecule the resonance does not come from the alignment of the HOMO and LUMO, since they cannot be decoupled through the conjugated $\pi-$bridge, but rather due to an asymmetric

voltage drop across the molecule [43]. Rectifying behavior in other classes of molecules is likely due to asymmetric contact with the electrodes [44, 45], or an asymmetry of the molecule itself [46]. To make rectifiers, one should avoid using molecules with long insulating groups, and we have suggested using relatively short molecules with "anchor" end groups for their self-assembly on a metallic electrodes, with a phenyl ring as a central conjugated part [47]. This idea has been tested in Ref. [48] with a phenyl and thiophene rings attached to a $(CH_2)_{15}$ tail by a CO group. The observed rectification ratio was $\leq$10, with some samples showing the ratio of about 37.

We have recently studied a more promising rectifier like $-$S-$(CH_2)_2$-Naph$-$ $(CH_2)_{10}-$S$-$ with a theoretical rectification $\leq 100$[49], Fig. 3. This system has been synthesized and studied experimentally [50]. To obtain an accurate description of transport in this case, we employ an ab-initio non-equilibrium Green's function method [51]. The present calculation takes into account only elastic tunneling processes. Inelastic processes may substantially modify the results in the case of strong interaction of the electrons with molecular vibrations, see Ref. [52] and below. There are indications in the literature that the carrier might be trapped in a polaron state in saturated molecules somewhat longer than those we consider in the present paper [53]. One of the barriers in the present rectifiers is short and relatively transparent, so there will be no appreciable Coulomb blockade effects. The structure of the present molecular rectifier is shown in Fig. 3. The molecule consists of a central conjugated part (naphthalene) isolated from the electrodes by two insulating aliphatic chains $(CH_2)_n$ with lengths $L_1(L_2)$ for the left (right) chain.

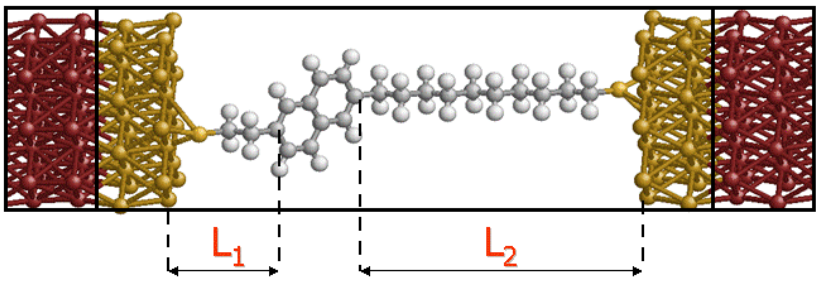


**Fig. 3.** Stick figure representing the naphthalene conjugated central unit separated from the left(right) electrode by saturated (wide band gap) alkane groups with length $L_{1(2)}$.

The principle of molecular rectification by a molecular quantum dot is illustrated in Fig. 4, where the electrically "active" molecular orbital, localized on the middle conjugated part, is the LUMO, which lies at an energy $\Delta$ above

the electrode Fermi level at zero bias. The position of the LUMO is determined by the work function of the metal $q\phi$ and the affinity of the molecule $q\chi$, $\Delta = \Delta_{\mathrm{LUMO}} = q\left(\phi - \chi\right)$. The position of the HOMO is given by $\Delta_{\mathrm{HOMO}} = \Delta_{\mathrm{LUMO}} - E_g$, where $E_g$ is the HOMO-LUMO gap. If this orbital is considerably closer to the electrode Fermi level $E_F$, then it will be brought into resonance with $E_F$ prior to other orbitals. It is easy to estimate the forward and reverse bias voltages, assuming that the voltage mainly drops on the insulating parts of the molecule,

$$V_F = \tfrac{\Delta}{q}(1+\xi), \qquad V_R = \tfrac{\Delta}{q}\left(1+\tfrac{1}{\xi}\right), \tag{2}$$

$$V_F/V_R = \xi \equiv L_1/L_2, \tag{3}$$

where $q$ is the elementary charge. A significant difference between forward and reverse currents should be observed in the voltage range $V_F < |V| < V_R$. The current is obtained from the Landauer formula

$$I = \frac{2q^2}{h}\int dE\left[f(E) - f(E+qV)\right] g(E,V). \tag{4}$$

We can make qualitative estimates in the resonant tunneling model, with the conductance $g(E,V) \equiv T(E,V)/q$, where $T(E,V)$ is the transmission given by the Breit-Wigner formula

$$T(E,V) = \frac{\Gamma_L \Gamma_R}{\left(E - E_{MO}\right)^2 + \left(\Gamma_L + \Gamma_R\right)^2/4}, \tag{5}$$

$E_{MO}$ is the energy of the molecular orbital. The width $\Gamma_{L(R)} \sim t^2/D = \Gamma_0 e^{-2\kappa L_{1(2)}}$, where $t$ is the overlap integral between the MO and the electrode, $D$ is the electron band width in the electrodes, $\kappa$ the inverse decay length of the resonant MO into the barrier. The current above the resonant threshold is

$$I \approx \frac{2q}{\hbar}\Gamma_0 e^{-2\kappa L_2}. \tag{6}$$

We see that increasing the spatial asymmetry of the molecule $(L_2/L_1)$ changes the operating voltage range linearly, but it also brings about an *exponential* decrease in current [47]. This severely limits the ability to optimize the rectification ratio while simultaneously keeping the resistance at a reasonable value. To calculate the I-V curves, we use an ab-initio approach that combines the Keldysh non-equilibrium Green's function (NEGF) with pseudopotential-based real space density functional theory (DFT) [51]. The main advantages of our approach are (i) a proper treatment of the open boundary condition; (ii) a fully atomistic treatment of the electrodes and (iii) a self-consistent calculation of the non-equilibrium charge density using NEGF. The transport Green's function is found from the Dyson equation

$$\left(G^R\right)^{-1} = \left(G_0^R\right)^{-1} - V, \tag{7}$$

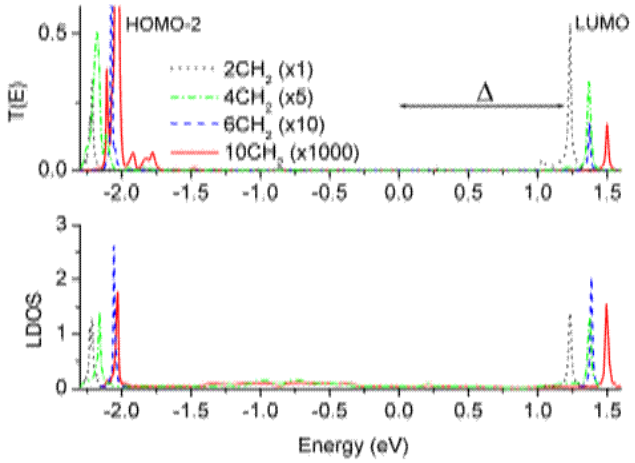


**Fig. 4.** Transmission coefficient versus energy E for rectifiers $-$S-$(CH_2)_2$-$C_{10}H_6-(CH_2)_n-$S$-$, $n = 2, 4, 6, 10$. $\Delta$ indicates the distance of the closest MO to the electrode Fermi energy ($E_F = 0$).

where the unperturbed retarded Green's function is defined in operator form as $\left(G_0^R\right)^{-1} = (E + i0)\hat{S} - \hat{H}$, $H$ is the Hamiltonian matrix for the scatterer (molecule plus screening part of the electrodes). $S$ is the *overlap* matrix, $S_{i,j} = \langle\chi_i|\chi_j\rangle$ for non-orthogonal basis set orbitals $\chi_i$, and the coupling of the scatterer to the leads is given by the Hamiltonian matrix $V = \mathrm{diag}[\Sigma_{l,l},\ 0,\ \Sigma_{r,r}]$, where $l$ ($r$) stands for left (right) electrode. The self-energy part $\Sigma^<$, which is used to construct the non-equilibrium electron density in the scattering region, is found from $\Sigma^< = -2i\mathrm{Im}\left[f(E)\Sigma_{l,l} + f(E + qV)\Sigma_{r,r}\right]$, where $\Sigma_{l,l(r,r)}$ is the self-energy of the left (right) electrode, calculated for the semi-infinite leads using an iterative technique [51]. $\Sigma^<$ accounts for the steady charge "flowing in" from the electrodes. The transmission probability is given by

$$T(E,V) = 4\mathrm{Tr}\left[\left(\mathrm{Im}\Sigma_{\mathrm{l,l}}\right) G^R_{l,r} \left(\mathrm{Im}\Sigma_{\mathrm{r,r}}\right) G^A_{r,l}\right], \tag{8}$$

where $G^{R(A)}$ are the retarded (advanced) Green's function, and $\Sigma$ the self-energy part connecting left ($l$) and right ($r$) electrodes [51], and the current is obtained from Eq. (4). The calculated transmission coefficient $T(E)$ is shown for a series of rectifiers $-$S-$(CH_2)_m$-$C_{10}H_6-(CH_2)_n-$S$-$ for $m = 2$ and $n = 2, 4, 6, 10$ at zero bias voltage in Fig. 4. We see that the LUMO is the molecular orbital transparent to electron transport, lies above $E_F$ by an amount $\Delta = 1.2 - 1.5$eV. The transmission through the HOMO and HOMO-1 states, localized on the terminating sulfur atoms, is negligible, but the HOMO-2 state conducts very well. The HOMO-2 defines the threshold reverse voltage $V_R$, thus limiting the operating voltage range. Our assumption, that the voltage drop is proportional to the lengths of the alkane groups on both sides, is

quantified by the calculated potential ramp. It is close to a linear slope along the $(CH_2)_n$ chains [49]. The forward voltage corresponds to the crossing of the LUMO($V$) and $\mu_R(V)$, which happens at about 2V. Although the LUMO defines the forward threshold voltages in all molecules studied here, the reverse voltage is defined by the HOMO-2 for "right" barriers $(CH_2)_n$ with $n = 6, 10$. The I-V curves are plotted in Fig. 5. We see that the rectification ratio for

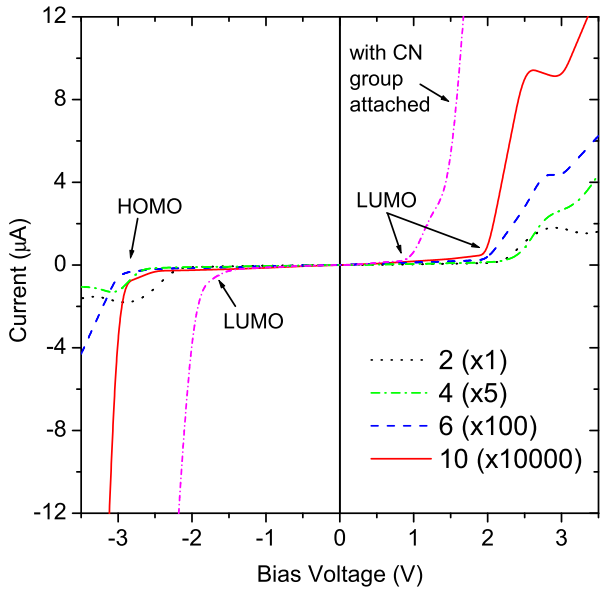


**Fig. 5.** I-V curves for naphthalene rectifiers $-$S-$(CH_2)_2$-$C_{10}H_6-(CH_2)_n-$S$-$, $n = 2, 4, 6, 10$. The short-dash-dot curve corresponds to a cyano-doped (added group -C≡N) $n = 10$ rectifier.

current in the operation window $I_+/I_-$ reaches a maximum value of 35 for the "2-10" molecule ($m = 2$, $n = 10$). Series of molecules with a central *single phenyl* ring [47] do not show any significant rectification. One can manipulate the system in order to increase the energy asymmetry of the conducting orbitals (reduce $\Delta$). To shift the LUMO towards $E_F$, one can attach an electron withdrawing group, like $-$C≡N [49]. The molecular rectification ratio is not great by any means, but one should bear in mind that this is a device necessarily operating in a ballistic quantum-mechanical regime because of the small size. This is very different from present Si devices with carriers diffusing through the system. As silicon devices become smaller, however, the same

effects will eventually take over, and tend to diminish the rectification ratio, in addition to effects of finite temperature and disorder in the system.

## 4 Molecular switches

There are various molecular systems that exhibit some kind of current "switching" behavior [34, 36, 37, 38], "negative differential resistance"[33], and "memory"[35]. The switching systems are basically driven between two states with considerably different resistances. This behavior is not really sensitive to a particular molecular structure, since this type of bistability is observed in complex rotaxane-like molecules as well as in very simple alkane chains $(CH_2)_n$ assembled into LB films [38], and is not even exclusive to the organic films. The data strongly indicates that the switching has an extrinsic origin, and is related either to bistability of molecule-electrode orientation [22, 23, 34], or transport assisted by defects in the film[54, 55].

### 4.1 Extrinsic switching in organic molecular films: role of defects and molecular reconfigurations

Evidently, large defects can be formed in organic thin films as a result of electromigration in very strong field, as was observed long ago[56]. It was concluded some decades ago that the conduction through absorbed [54] and Langmuir-Blodgett [55] monolayers of fatty acids $(CH_2)_n$, which we denote as Cn, is associated with *defects*. In particular, Polymeropoulos and Sagiv studied a variety of absorbed monolayers from C7 to C23 on $Al/Al_2O_3$ substrates and found that the exponential dependence on the length of the molecular chains is only observed below the liquid nitrogen temperature of 77K, and no discernible length dependence was observed at higher temperatures [54]. The temperature dependence of current was strong, and was attributed to transport assisted by some defects. The current also varied strongly with the temperature in Ref. [55] for LB films on $Al/Al_2O_3$ substrates in He atmosphere, which is not compatible with elastic tunneling. Since the He atmosphere was believed to hinder the $Al_2O_3$ growth, and yet the resistance of the films increased about 100-fold over 45 days, the conclusion was made that the "defects" somehow anneal out with time. Two types of switching have been observed in 3-30 $\mu$m thick films of polydimethylsiloxane (PDMS), one as a standard dielectric breakdown with electrode material "jet evaporation" into the film with subsequent Joule melting of metallic filament under bias of about 100V, and a low-voltage (<1 V) "ultraswitching" that has a clear "telegraph" character and resulted in intermittent switching into a much more conductive state[57]. The exact nature of this switching also remains unclear, but there is a strong expectations that the formation of metallic filaments that may even be in a ballistic regime of transport, may be relevant to the phenomenon.

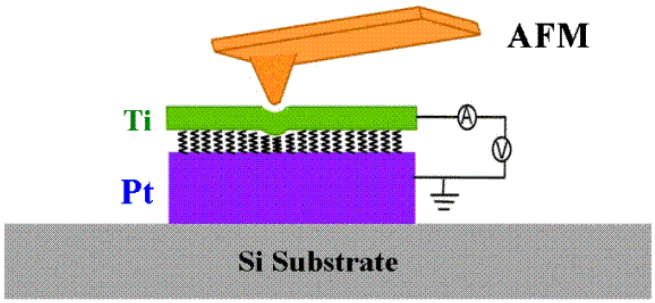


**Fig. 6.** Experimental setup for mapping local conductance. AFM produces local deformation of top electrode and underlying organic film. The *total* conductance of the device is measured and mapped. (Courtesy C.N. Lau).

Recently, a direct evidence was obtained of the formation of "hot spots" in the LB films that may be related to the filament growth through the film imaged with the use of AFM current mapping[58]. The system investigated in this work has been Pt/stearic acid (C18)/Ti (Pt/C18/Ti) crossbar molecular structure, consisting of planar Pt and Ti electrodes sandwiching a monolayer of 2.6-nm-long stearic acid (C18H36OH) molecules with typical zero-bias resistance in excess of $10^5\Omega$. The devices has been switched reversibly and repeatedly to higher ("on") or lower ("off") conductance states by applying sufficiently large bias voltage $V_b$ to top Ti electrode with regards to Pt counterelectrode, Fig. 6.

Interestingly, reversible switching was not observed in symmetric Pt/C18/Pt devices. The local conductance maps of the Pt/C18/Ti structure have been constructed by using an AFM tip and simultaneously measuring the current through the molecular junction biased to $V_b = 0.1$V (AFM tip was not used as an electrode, only to apply local pressure at the surface). The study revealed that the film showed pronounced switching between electrically very distinct states, with zero-bias conductances $0.17\mu$S ("off" state) and $1.45\mu$S ("on" state), Fig. 7.

At every switching "on" there appeared a local conductance peak on the map with a typical diameter $\sim 40$nm, which then disappeared upon switching "off", Fig. 7 (top inset). The switching has been attributed to local conducting filament formation due to electromigration processes. It remains unclear how exactly the filaments dissolve under opposite bias voltage, why they tend to appear in new places after each switching, and why conductance in some cases strongly depends on temperature. It is clear, however, that switching in such a simple molecule without any redox centers, mobile groups, or charge reception centers should be *extrinsic*. Interestingly, very similar "switching" between two resistive states has also been observed for tunneling through thin *inorganic* perovskite oxide films[59].

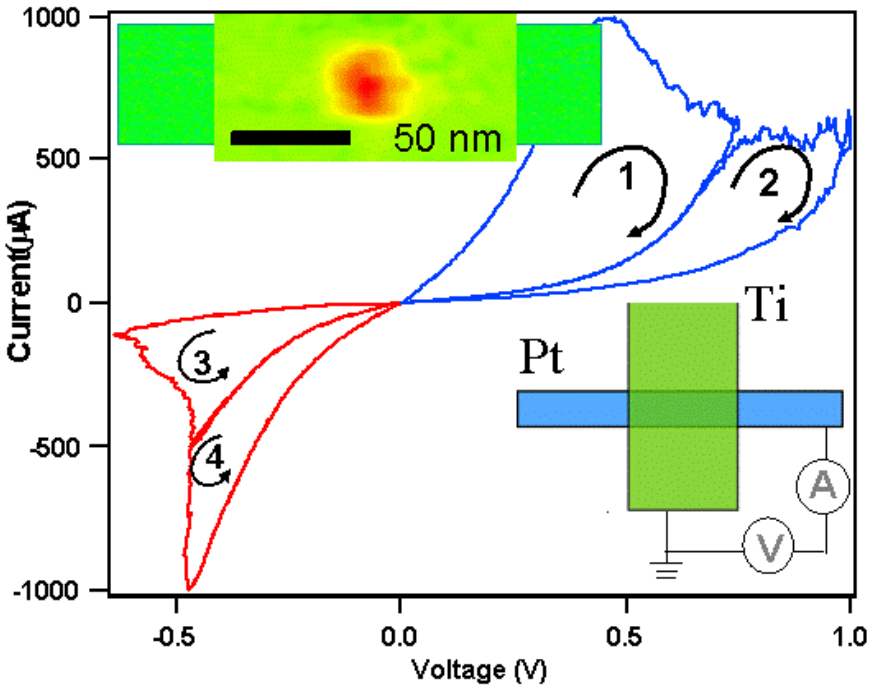


**Fig. 7.** I-V characteristic showing the reversible switching cycle of the device (bottom inset) with organic film. The arrows indicate sweep direction. A negative bias switches the device to a high conductance state, while the positive one switches it to low conductance state. The mapping according the schematic in Fig. 6 shows the appearance of "hot spots" after switching (top inset). (Courtesy C.N. Lau).

There have been plenty of reports on non-linear I-V characteristics like negative differential resistance (NDR) and random switching recently for molecules assembled on metal electrodes (gold) and silicon. Reports on NDR for molecules with metal contacts (Au, Hg) have been made in [33, 45, 60]. It became very clear though that most of these observations are related to molecular reconfigurations and bond breaking and making, rather to any intrinsic mechanism, like redox states, speculated about in the original Ref. [33]. Thus, the NDR in Tour wires was related to molecular reconfiguration with respect to metallic electrode[22, 34], NDR in ferrocene-tethered alkyl monolayers [60] was found to be related to oxygen damage at high voltage[61]. Structural changes and bond breaking have been found to result in NDR in experiments with STM [62, 63, 64] and mercury droplet contacts[65].

Several molecules, like styrene, have been studied on degenerate Si surface and showed an NDR behavior[66]. However, those results have been carefully

checked later and it was found that the styrene molecules do not exhibit NDR, but rather sporadically switch between states with different current while held at the same bias voltage (the blinking effect) [67].

The STM map of the styrene molecules (indicated by arrows) on the Silicon (100) surface shows that the molecules are blinking, see Fig. 8. The blinking is absent at clean Si areas, dark (D) and bright (C) defects. This may indicate a dynamic process occurring during the imaging. Comparing the panel (a) and (b) one may see that some molecules are actually decomposing. The height versus voltage spectra over particular points are shown in Fig. 8c. The featureless curve 1 was taken over a clean silicon dimer. The other spectra were recorded over individual molecules. Each of these spectra have many sudden decreases and increases in current as if the molecules are changing between different states during the measurement causing a change in current and a response of the feedback control, resulting in a change in height so there exists one or more configurations that lead to measurement of a different height. Evidently, these changes have the same origin as the blinking of molecules in STM images. Figure 8b reveals clear structural changes associated with those particular spectroscopic changes. In each case where a dramatic change in spectroscopy occurred, the molecules in the image have changed from a bright feature to a dark spot. This is interpreted as a decomposition of the molecules. A detailed look at each decomposed styrene molecule, at locations 3, 4, 5, and 6, shows that the dark spot is not in precise registry with the original bright feature, indicating that the decomposition product involves reaction with an adjacent dimer[67].

The fact that the structural changes and related NDR behavior are not associated with any resonant tunneling through the molecular levels or redox processes, but are perhaps related to inelastic electron scattering or other extrinsic processes, becomes evident from current versus time records shown in Fig. 9, Ref.[67]. The records show either no change of the current with time (1), or one or a few random jumps between certain current states (telegraph noise). The observed changes in current at a fixed voltage obviously cannot be explained by shifting and aligning of molecular levels, as was suggested in Ref. [68], they must be related to an adsorbate molecule structural changes with time. Therefore, the explanation by Datta *et al.* that the resonant level alignment is responsible for NDR does not apply[68]. As mentioned above, similar telegraph switching and NDR has been observed in Tour wires[34] and other molecules. Therefore, the observed negative differential resistance apparently has similar origin in disparate molecules adsorbed on different substrates, and has to do with molecular reconformation/reconfiguration on the surface.

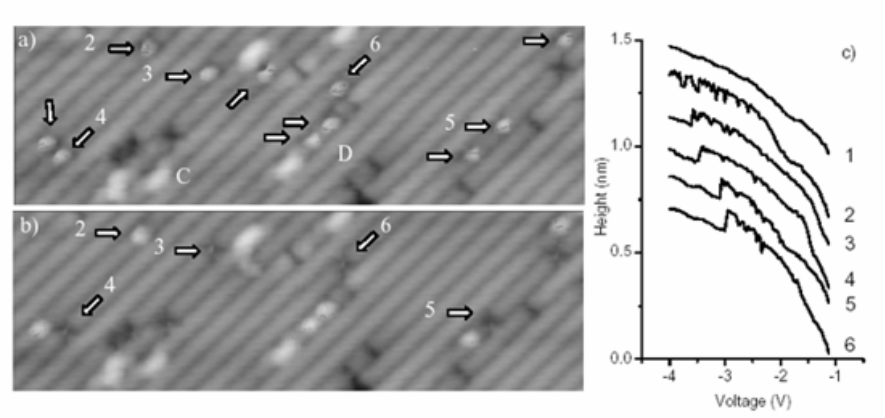


**Fig. 8.** STM images or styrene molecules on clean Si(100) before and after spectroscopy over the area 75 ×240 Å. (Top left) Bias -2 V, current 0.7 nA. Only the styrene molecules (indicated by arrows) are blinking during imaging. The clean Si surface, bright defects (marked C), and dark sports (marked D) do not experience blinking. (Bottom left) bias -2 V, current 0.3 nA. STM image of individual styrene molecules indicated with numbers 2-6. Styrene molecules 3-6 have decomposed. Decomposition involves the changing of the styrene molecule from a bright feature to a dark depression and also involves the reaction with an adjacent dimer. Styrene molecule 2 does not decompose and images as usual with no change of position. (Right) Height-voltage spectra taken over clean silicon (1) and styrene molecules (2-6). The spectra taken over molecules show several spikes in height related to blinking in the images. In spectra 3-6, an abrupt and permanent change in height is recorded and is correlated with decomposition, as seen in the bottom left image. Spectrum 2 has no permanent height change, and the molecule does not decompose. (Courtesy J. Pitters and R. Wolkow).

### 4.2 Intrinsic polarization and extrinsic conductance switching in molecular ferroelectric PVDF

The only well established, to the best of our knowledge, intrinsic molecular switching (of polarization, not current) under bias voltage was observed in molecular ferroelectric block co-polymers polyvinylidene[69]. Ferroelectric polymer films have been prepared with the 70% vinylidene fluoride copolymer, P(VDF-TrFE 70:30), formed by horizontal LB deposition on aluminum-coated glass substrates with evaporated aluminum top electrodes. The polymer chains contain random sequence of $(CH_2)_n(CF_2)_m$ blocks, fluorine site carries a strong negative charge, and in the ferroelectric phase most of carbon-fluorine bonds point in one direction. The fluorine groups can be rotated and aligned in very strong electric field, $\sim$ 5MV/cm. As a result, the whole molecular chain orders, and in this way the macroscopic polarization can be switched between the opposite states. The switching process is extremely slow, how-

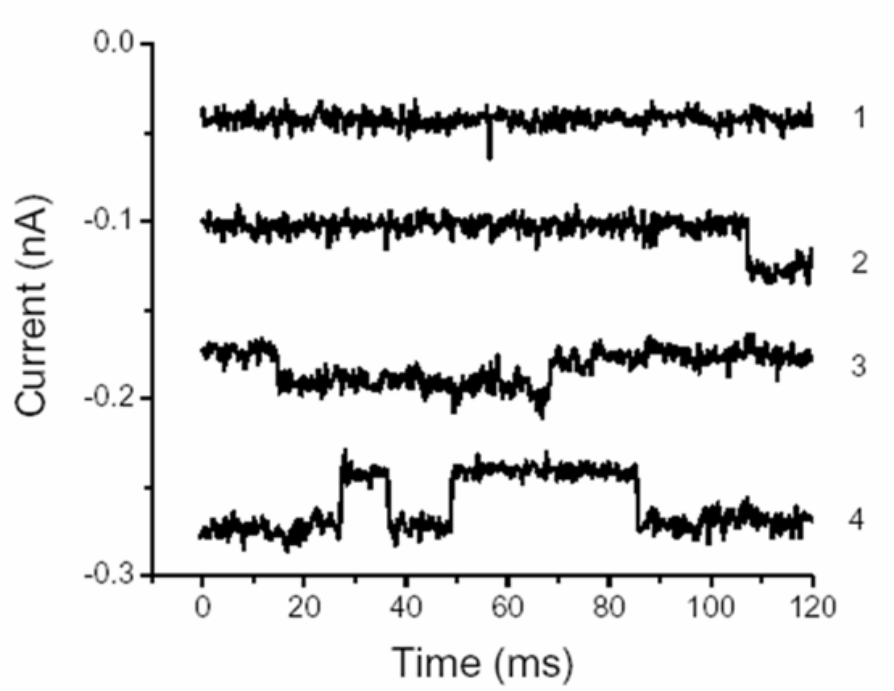


**Fig. 9.** Variation of current through styrene molecules on Si(100) with time. Tunneling conditions were set at -3 V and 0.05 nA. Abrupt increases and decreases in current relate to changes of the molecule during the spectroscopy. Some experiments show no changes in current (curve 1), others show various kinds of telegraph switching. (Courtesy J. Pitters and R. Wolkow).

ever, and takes 1-10 seconds (!) [70, 71]. This is not surprising, given strong Coulomb interaction between charged groups and the metal electrodes, pinning by surface roughness, and steric hindrance to rotation. This behavior should be suggestive of other switching systems based on one of few monolayers of molecules, and other nontrivial behavior involved[71].

The switching of current was also observed in films of PVDF 30 monolayers thick. The conductance of the film was following the observed hysteresis loop for the polarization, ranging from $\sim 1 \times 10^{-9} - 2 \times 10^{-6} \Omega^{-1}$[72]. The phenomenon of conductance switching has these important features: (i) It is connected with the bulk polarization switching; (ii) there is a large $\sim 1000 : 1$ contrast between the ON and OFF states; (iii) the ON state is obtained only when the bulk polarization is switched in the positive direction; (iv) the conductance switching is much faster than the bulk polarization switching. The conductance switches ON only after the 6s delay, after the bulk polarization switching is nearly complete, presumably when the last layer switches into

alignment with the others, while the conductance switches OFF without a noticeable delay after the application of reverse bias as even one layer reverses (this may create a barrier to charge transfer). The slow $\sim$ 2s time constant for polarization switching is probably nucleation limited as has been observed in high-quality bulk films with low nucleation site densities[73]. The duration of the conductance switching transition $\sim$ 2ms may be limited only by the much faster switching time of individual layers.

The origin of conductance switching by 3 orders of magnitude is not clear. It may indeed be related to a changing amount of disorder for tunneling/hopping electrons. It is conceivable that the carriers are strongly trapped in polaron states inside PVDF and find optimal path for hopping in the material, which is incompletely switched. This is an interesting topic that certainly in need of further experimental and theoretical study.

## 5 Molecular quantum dot switching

### 5.1 Electrically addressable molecules

For many applications one needs an *intrinsic* molecular "switch", i.e. a bistable voltage-addressable molecular system with very different resistances in the two states that can be accessed very quickly. There is a trade-off between the stability of a molecular state and the ability to switch the molecule between two states with an external perturbation (we discuss an electric field, switching involving absorbed photons is impractical at a nanoscale). Indeed, the applied electric field, on the order of a typical breakdown field $E_b \leq 10^7$V/cm, is much smaller than a typical atomic field $\sim 10^9$V/cm, characteristic of the energy barriers. Small barrier would be a subject for sporadic thermal switching, whereas a larger barrier $\sim 1-2$eV would be impossible to overcome with the applied field. One may only change the relative energy of the minima by external field and, therefore, redistribute the molecules statistically slightly inequivalently between the two states. An intrinsic disadvantage of the conformational mechanism, involving motion of ionic group, exceeding the electron mass by many orders of magnitude, is a slow switching speed ($\sim$kHz). In case of supramolecular complexes like rotaxanes and catenanes [36] there are two entangled parts which can change mutual positions as a result of redox reactions (in solution). Thus, for the rotaxane-based memory devices a slow switching speed of $\sim 10^{-2}$ seconds was reported.

As a possible conformational $E$-field addressable molecular switch, we have considered a bistable molecule with -$CONH_2$ dipole group [74]. The barrier height is $E_b = 0.18$eV. Interaction with an external electric field changes the energy of the minima, but estimated switching field is huge, $\sim 0.5$V/A. At non-zero temperatures, temperature fluctuations might result in statistical dipole flipping at lower fields. The I-V curve shows hysteresis in the 3 to 4

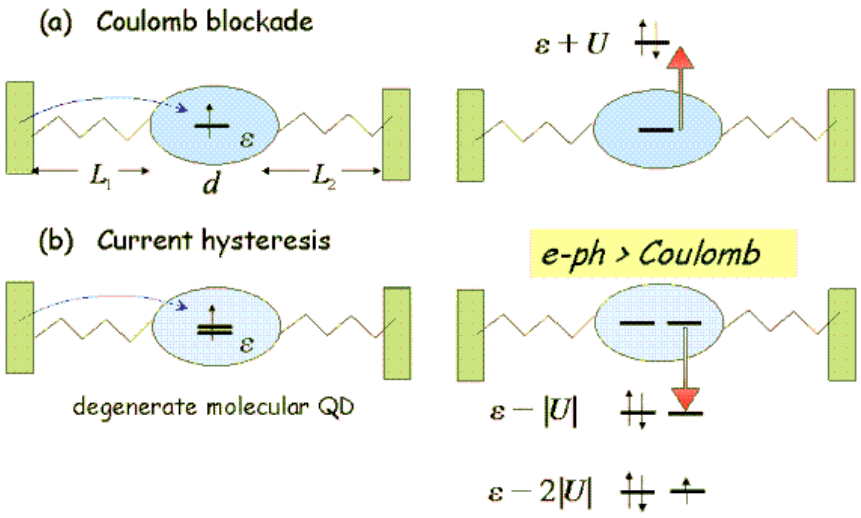


**Fig. 10.** Schematic of the molecular quantum dot with central conjugated unit separated from the electrodes by wide-band insulating molecular groups. First electron tunnels into the dot and occupies an empty (degenerate) state there. If the interaction between the first and second incoming electron is repulsive, $U > 0$, then the dot will be in a Coulomb blockade regime (a). If the electrons on the dot effectively attract each other, $U < 0$, the system will show current hysteresis (b).

Volts window for two possible conformations. One can estimate the thermal stability of the state as 58 ps at room temperature, and 33 ms at 77 K.

We explored a possibility for a fast molecular switching where switching is due to strong correlation effects on the molecule itself, so-called molecular quantum dot (MQD). The molecular quantum dot consists of a central *conjugated* unit (containing half-occupied, and, therefore, extended $\pi-$orbitals), Fig. 10. Frequently, those are formed from the p-states on carbon atoms, which are not *saturated* (i.e. they do not share electrons with other atoms forming strong $\sigma-$bonds, with typical bonding-antibonding energy difference about 1Ry). Since the $\pi-$orbitals are half-occupied, they form the HOMO-LUMO states. The size of the HOMO-LUMO gap is then directly related to the size of the conjugated region $d$, Fig. 10, by a standard estimate $E_{\text{HOMO-LUMO}} \sim \hbar^2/md^2 \sim 2-5$ eV. It is worth noting that in the conjugated linear polymers like polyacetylene $(-\overset{|}{C} = \overset{|}{C})_n$ the spread of the $\pi-$electron would be $d = \infty$ and the expected $E_{\text{HOMO-LUMO}} = 0$. However, such a one-dimensional metal is impossible, Peierls distortion (C=C bond length dimerization) sets in and opens up a gap of about $\sim 1.5$eV at the Fermi level[17]. In a molecular quantum dot the central conjugated part is

separated from electrodes by insulating groups with saturated $\sigma-$bonds, like e.g. the alkane chains, Fig. 3. Now, there are two main possibilities for carrier transport through the molQD. If the length of at least one of the insulating groups $L_{1(2)}$ is not very large (a conductance $G_{1(2)}$ is not much smaller than the conductance quantum $G_0 = 2e^2/h$), then the transport through the MQD will proceed by resonant tunneling processes. If, on the other hand, both groups are such that the tunnel conductance $G_{1(2)} \ll G_0$, the charge on the dot will be quantized. Then we will have another two possibilities: (i) the interaction of the extra carriers on the dot is *repulsive* $U > 0$, and we have a Coulomb blockade [75], or (ii) the effective interaction is *attractive*, $U < 0$, then we would obtain the current *hysteresis* and switching (see below). Coulomb blockade in molecular quantum dots has been demonstrated in Refs. [76]. In these works, and in Ref. [77], the three-terminal active molecular devices have been fabricated and successfully tested.

Much faster switching compared to the conformational one, described in the previous section, may be caused by coupling to the vibrational degrees of freedom, if the vibron-mediated attraction between two carriers on the molecule is stronger than their direct Coulomb repulsion [52], Fig. 10b. The attractive energy is the difference of two large interactions, the Coulomb repulsion and the phonon mediated attraction, on the order of 1eV each, hence $|U| \sim 0.1$eV.

### 5.2 Polaron mechanism of carrier attraction and switching

Although the correlated electron transport through mesoscopic systems with repulsive electron-electron interactions received considerable attention in the past, and continues to be the focus of current studies, much less has been known about a role of electron-phonon correlations in "molecular quantum dots" (MQD). Some while ago we have proposed a negative$-U$ Hubbard model of a $d$-fold degenerate quantum dot [78] and a polaron model of resonant tunneling through a molecule with degenerate level [52]. We found that the *attractive* electron correlations caused by any interaction within the molecule could lead to a molecular *switching* effect where I-V characteristics have two branches with high and low current at the same bias voltage. This prediction has been confirmed and extended further in our theory of *correlated* transport through degenerate MQDs with a full account of both the Coulomb repulsion and realistic electron-phonon (e-ph) interactions [52]. We have shown that while the phonon side-bands significantly modify the shape of hysteretic I-V curves in comparison with the negative-$U$ Hubbard model, switching remains robust. It shows up when the effective interaction of polarons is attractive and the state of the dot is multiply degenerate, $d > 2$.

First, we shall describe a simplest model of a single atomic level coupled with a single one-dimensional oscillator using the first quantization representation for its displacement $x$ [79],

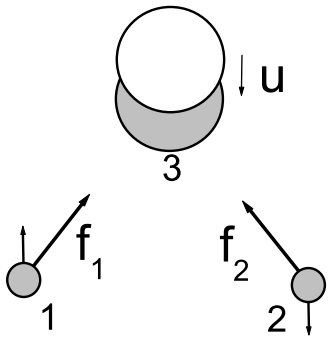


**Fig. 11.** Two localized electrons at sites **1** and **2** with opposite spins shift the equilibrium position of the ion at site **3**. As a result, the two electrons *attract* each other.

$$H = \varepsilon_0 \hat{n} + fx\hat{n} - \frac{1}{2M}\frac{\partial^2}{\partial x^2} + \frac{kx^2}{2}. \tag{9}$$

Here $M$ and $k$ are the oscillator mass and the spring constant, $f$ is the interaction force, and $\hbar = c = k_B = 1$. This Hamiltonian is readily diagonalized with the *exact* displacement transformation of the vibration coordinate $x$,

$$x = y - \hat{n}f/k, \tag{10}$$

to the transformed Hamiltonian without electron-phonon coupling,

$$\tilde{H} = \varepsilon\hat{n} - \frac{1}{2M}\frac{\partial^2}{\partial y^2} + \frac{ky^2}{2}, \tag{11}$$

$$\varepsilon = \varepsilon_0 - E_p, \tag{12}$$

where we used $\hat{n}^2 = \hat{n}$ because of the Fermi-Dirac statistics. It describes a small polaron at the atomic level $\varepsilon_0$ shifted down by the polaron level shift $E_p = f^2/2k$, and entirely decoupled from ion vibrations. The ion vibrates near a new equilibrium position, shifted by $f/k$, with the "old" frequency $(k/M)^{1/2}$. As a result of the local ion deformation, the total energy of the whole system decreases by $E_p$ since a decrease of the electron energy by $-2E_p$ overruns an increase of the deformation energy $E_p$. Note that the authors of Ref. [80] made an illegitimate replacement of the square of the occupation number operator

$\hat{n} = c_0^\dagger c_0$ in Eq. (11) by its "mean-field" expression $\hat{n}^2 = n_0\hat{n}$ which contains the average population of a single molecular level, $n_0$, in disagreement with the exact identity, $\hat{n}^2 = \hat{n}$. This leads to a spurious *self-interaction* of a single polaron with itself [i.e. the term $\varepsilon = \varepsilon_0 - n_0 E_p$ instead of Eq. (12)], and a resulting non-existent nonlinearity in the rate equation.

Lattice deformation also strongly affects the interaction between electrons. When a short-range deformation potential and molecular e-ph interactions are taken into account together with the long-range Fröhlich interaction, they can overcome the Coulomb repulsion. The resulting interaction becomes attractive at a short distance comparable to a lattice constant. The origin of the attractive force between two small polarons can be readily understood from a similar Holstein-like toy model as above [81], but with two electrons on neighboring sites **1,2** interacting with an ion **3** between them, Fig. 11. For generality, we now assume that the ion is a three-dimensional oscillator described by a displacement vector $\mathbf{u}$, rather than by a single-component displacement $x$ as in Eq.(1).

The vibration part of the Hamiltonian in the model is

$$H_{ph} = -\frac{1}{2M}\frac{\partial^2}{\partial \mathbf{u}^2} + \frac{k\mathbf{u}^2}{2}, \tag{13}$$

Electron potential energies due to the Coulomb interaction with the ion are about

$$V_{1,2} = V_0 - \mathbf{u}\nabla_{R_{1,2}} V_0(R_{1,2}), \tag{14}$$

where $\mathbf{R_{1(2)}}$ is the vector connecting ion site **3** with electron **1**(**2**). Hence, the Hamiltonian of the model is given by

$$H = E_a(\hat{n}_1 + \hat{n}_2) + \mathbf{u}\cdot(\mathbf{f_1}\hat{n}_1 + \mathbf{f_2}\hat{n}_2) - \frac{1}{2M}\frac{\partial^2}{\partial \mathbf{u}^2} + \frac{k\mathbf{u}^2}{2}, \tag{15}$$

where $\mathbf{f_{1,2}} = Ze^2\mathbf{e_{1,2}}/a^2$ is the Coulomb force, and $\hat{n}_{1,2}$ are occupation number operators at every site. This Hamiltonian is also readily diagonalized by the same displacement transformation of the vibronic coordinate $\mathbf{u}$ as above,

$$\mathbf{u} = \mathbf{v} - (\mathbf{f_1}\hat{n}_1 + \mathbf{f_2}\hat{n}_2)/k. \tag{16}$$

The transformed Hamiltonian has no electron-phonon coupling,

$$\tilde{H} = (\varepsilon_0 - E_p)(\hat{n}_1 + \hat{n}_2) + V_{ph}\hat{n}_1\hat{n}_2 - \frac{1}{2M}\frac{\partial^2}{\partial \mathbf{v}^2} + \frac{k\mathbf{v}^2}{2}, \tag{17}$$

and it describes two small polarons at their atomic levels shifted by the polaron level shift $E_p = f_{1,2}^2/2k$, which are entirely decoupled from ion vibrations. As a result, the lattice deformation caused by two electrons leads to an effective interaction between them, $V_{ph}$, which should be added to their Coulomb repulsion, $V_c$,

$$V_{ph} = -\mathbf{f_1}\cdot\mathbf{f_2}/k. \tag{18}$$

When $V_{ph}$ is negative and larger by magnitude than the positive $V_c$, the resulting interaction becomes attractive. That is $V_{ph}$ rather than $E_p$, which is responsible for the hysteretic behavior of MQDs, as discussed below.

### 5.3 Exact solution

The procedure, which fully accounts for all correlations in MQD is as follows, see Ref. [52]. The molecular Hamiltonian includes the Coulomb repulsion, $U^C$, and the electron-vibron interaction as

$$H = \sum_{\mu} \varepsilon_{\mu} \hat{n}_{\mu} + \frac{1}{2} \sum_{\mu \neq \mu'} U^C_{\mu\mu'} \hat{n}_{\mu} \hat{n}_{\mu'} + \sum_{\mu,q} \hat{n}_{\mu} \omega_q (\gamma_{\mu q} d_q + H.c.) + \sum_{q} \omega_q (d_q^{\dagger} d_q + 1/2). \tag{19}$$

Here $d_q$ annihilates phonons, $\omega_q$ is the phonon (vibron) frequency, and $\gamma_{\mu q}$ are the e-ph coupling constant ($q$ enumerates the vibron modes). This Hamiltonian conserves the occupation numbers of molecular states $\hat{n}_{\mu}$.

One can apply the canonical unitary transformation $e^S$, with

$$S = -\sum_{q,\mu} \hat{n}_{\mu} \left( \gamma_{\mu q} d_q - H.c. \right)$$

integrating phonons out. The electron and phonon operators are transformed as

$$\tilde{c}_{\mu} = c_{\mu} X_{\mu}, \qquad X_{\mu} = \exp\left( \sum_{q} \gamma_{\mu q} d_q - H.c. \right) \tag{20}$$

and

$$\tilde{d}_q = d_q - \sum_{\mu} \hat{n}_{\mu} \gamma^*_{\mu q}, \tag{21}$$

respectively. This Lang-Firsov transformation shifts ions to new equilibrium positions with no effect on the phonon frequencies. The diagonalization is *exact*:

$$\tilde{H} = \sum_{i} \tilde{\varepsilon}_{\mu} \hat{n}_{\mu} + \sum_{q} \omega_q (d_q^{\dagger} d_q + 1/2) + \frac{1}{2} \sum_{\mu \neq \mu'} U_{\mu\mu'} \hat{n}_{\mu} \hat{n}_{\mu'}, \tag{22}$$

where

$$U_{\mu\mu'} \equiv U^C_{\mu\mu'} - 2 \sum_{q} \gamma^*_{\mu q} \gamma_{\mu' q} \omega_q, \tag{23}$$

is the renormalized interaction of polarons comprising their interaction via molecular deformations (vibrons) and the original Coulomb repulsion, $U^C_{\mu\mu'}$. The molecular energy levels are shifted by the polaron level-shift due to the deformation created by the polaron,

$$\tilde{\varepsilon}_{\mu} = \varepsilon_{\mu} - \sum_{q} |\gamma_{\mu q}|^2 \omega_q. \tag{24}$$

If we assume that the coupling to the leads is weak, so that the level width $\Gamma \ll |U|$, we can find the current from [82]

$$I(V) = I_0 \int_{-\infty}^{\infty} d\omega \left[ f_1(\omega) - f_2(\omega) \right] \rho(\omega), \tag{25}$$

$$\rho(\omega) = -\frac{1}{\pi} \sum_{\mu} \mathrm{Im} \hat{G}^R_{\mu}(\omega), \tag{26}$$

where $|\mu\rangle$ is a complete set of one-particle molecular states, $f_{1(2)}(\omega) = \left( \exp \frac{\omega + \Delta \mp eV/2}{T} + 1 \right)^{-1}$ the Fermi function. Here $I_0 = q\Gamma$, $\rho(\omega)$ is the molecular DOS, $\hat{G}^R_{\mu}(\omega)$ is the Fourier transform of the Green's function $\hat{G}^R_{\mu}(t) = -i\theta(t) \left\langle \left\{ c_{\mu}(t), c^{\dagger}_{\mu} \right\} \right\rangle$, $\{ \cdots, \cdots \}$ is the anticommutator, $c_{\mu}(t) = e^{iHt} c_{\mu} e^{-iHt}$, $\theta(t) = 1$ for $t > 0$ and zero otherwise. We calculate $\rho(\omega)$ *exactly* for the Hamiltonian (22), which includes both the Coulomb $U^C$ and e-ph interactions.

The retarded GF becomes

$$\begin{aligned} G^R_{\mu}(t) = -i\theta(t) [ & \left\langle c_{\mu}(t) c^{\dagger}_{\mu} \right\rangle \left\langle X_{\mu}(t) X^{\dagger}_{\mu} \right\rangle \\ & + \left\langle c^{\dagger}_{\mu} c_{\mu}(t) \right\rangle \left\langle X^{\dagger}_{\mu} X_{\mu}(t) \right\rangle ]. \end{aligned} \tag{27}$$

The phonon correlator is simply

$$\begin{aligned} \left\langle X_{\mu}(t) X^{\dagger}_{\mu} \right\rangle = & \exp \sum_{q} \frac{|\gamma_{\mu q}|^2}{\sinh \frac{\beta \omega_q}{2}} \\ & \times \left[ \cos \left( \omega t + i \frac{\beta \omega_q}{2} \right) - \cosh \frac{\beta \omega_q}{2} \right], \end{aligned} \tag{28}$$

where the inverse temperature $\beta = 1/T$, and $\left\langle X^{\dagger}_{\mu} X_{\mu}(t) \right\rangle = \left\langle X_{\mu}(t) X^{\dagger}_{\mu} \right\rangle^*$. The remaining GFs $\left\langle c_{\mu}(t) c^{\dagger}_{\mu} \right\rangle$, are found from the equations of motion *exactly*. Finally, for the simplest case of a coupling to a single mode with the characteristic frequency $\omega_0$ and $\gamma_q \equiv \gamma$ we find [52]

$$\begin{aligned} G^R_{\mu}(\omega) = & \mathcal{Z} \sum_{r=0}^{d-1} C_r(n) \sum_{l=0}^{\infty} I_l(\xi) \\ & \left[ e^{\frac{\beta \omega_0 l}{2}} \left( \frac{1-n}{\omega - rU - l\omega_0 + i\delta} + \frac{n}{\omega - rU + l\omega_0 + i\delta} \right) \right. \\ & + (1 - \delta_{l0}) e^{-\frac{\beta \omega_0 l}{2}} \\ & \left. \times \left( \frac{1-n}{\omega - rU + l\omega_0 + i\delta} + \frac{n}{\omega - rU - l\omega_0 + i\delta} \right) \right], \end{aligned} \tag{29}$$

where

$$\mathcal{Z} = \exp\left(-\sum_{\mathbf{q}} |\gamma_q|^2 \coth\frac{\beta\omega_q}{2}\right) \tag{30}$$

is the familiar *polaron narrowing* factor, the degeneracy factor

$$C_r(n) = \frac{(d-1)!}{r!(d-1-r)!} n^r (1-n)^{d-1-r}, \tag{31}$$

$\xi = |\gamma|^2/\sinh\frac{\beta\omega_0}{2}$, $I_l(\xi)$ the modified Bessel function, and $\delta_{lk}$ the Kroneker symbol. The important feature of the DOS, Eq. (25), is its nonlinear dependence on the occupation number $n$. It contains full information about all possible correlation and inelastic effects in transport, in particular, all the phonon sidebands.

To simplify our discussion, we assume that the Coulomb integrals do not depend on the orbital index, i.e. $U_{\mu\mu'} = U$, and consider a coupling to a single vibrational mode, $\omega_q = \omega_0$. Applying the same transformation to the retarded Green's function, one obtains the exact spectral function [52] for a $d-$ fold degenerate MQD (i.e. the density of molecular states, DOS) as

$$\begin{aligned}\rho(\omega) &= \mathcal{Z}d\sum_{r=0}^{d-1} C_r(n)\sum_{l=0}^{\infty} I_l(\xi)\\ &\times\Big[e^{\beta\omega_0 l/2}\left[(1-n)\delta(\omega-rU-l\omega_0)+n\delta(\omega-rU+l\omega_0)\right]\\ &+(1-\delta_{l0})e^{-\beta\omega_0 l/2}[n\delta(\omega-rU-l\omega_0)\\ &+(1-n)\delta(\omega-rU+l\omega_0)]\Big],\end{aligned} \tag{32}$$

where $\mathcal{Z} = \exp\left[-|\gamma|^2\coth\frac{\beta\omega_0}{2}\right]$, is the above polaron narrowing factor, $\xi = |\gamma|^2/\sinh(\beta\omega_0/2)$, $\beta = 1/T$, and $\delta_{lk}$ the Kroneker symbol.

The important feature of DOS, Eq. (32), is its nonlinear dependence on the average electronic population $n = \left\langle c_\mu^\dagger c_\mu\right\rangle$, which leads to the switching, hysteresis, and other nonlinear effects in I-V characteristics for $d > 2$ [52]. It appears due to *correlations* between *different* electronic states via the correlation coefficients $C_r(n)$. There is no nonlinearity if the dot is nondegenerate, $d = 1$, since $C_0(n) = 1$. In this simple case the DOS, Eq. (32), is a *linear* function of the average population that can be found as a textbook example of an exactly solvable problems [83].

In the present case of MQD weakly coupled with leads, one can apply the Fermi-Dirac golden rule to obtain an equation for $n$. Equating incoming and outgoing numbers of electrons in MQD per unit time we obtain the self-consistent equation for the level occupation $n$ as

$$(1-n)\int_{-\infty}^{\infty} d\omega \left\{\Gamma_1 f_1(\omega) + \Gamma_2 f_2(\omega)\right\}\rho(\omega)$$
$$= n\int_{-\infty}^{\infty} d\omega \left\{\Gamma_1[1-f_1(\omega)] + \Gamma_2[1-f_2(\omega)]\right\}\rho(\omega), \tag{33}$$

where $\Gamma_{1(2)}$ are the transition rates from left (right) leads to MQD, and $\rho(\omega)$ is found from Eqs. (29) and (25). For $d = 1, 2$ the kinetic equation for $n$ is linear, and the switching is *absent.* Switching appears for $d \geq 3$, when the kinetic equation becomes non-linear. Taking into account that $\int_{-\infty}^{\infty}\rho(\omega) = d$, Eq. (33) for the symmetric leads, $\Gamma_1 = \Gamma_2$, reduces to

$$2nd = \int d\omega\rho\left(\omega\right)\left(f_1 + f_2\right), \tag{34}$$

which automatically satisfies $0 \leq n \leq 1$. Explicitly, the self-consistent equation for the occupation number is

$$n = \frac{1}{2}\sum_{r=0}^{d-1} C_r(n)[na_r^+ + (1-n)b_r^+], \tag{35}$$

where

$$a_r^+ = \mathcal{Z}\sum_{l=0}^{\infty} I_l\left(\xi\right)\Big(e^{\frac{\beta\omega_0 l}{2}}[f_1(rU - l\omega_0) + f_2(rU - l\omega_0)]$$
$$+(1-\delta_{l0})e^{-\frac{\beta\omega_0 l}{2}}[f_1(rU + l\omega_0) + f_2(rU + l\omega_0)]\Big), \tag{36}$$

$$b_r^+ = \mathcal{Z}\sum_{l=0}^{\infty} I_l\left(\xi\right)\Big(e^{\frac{\beta\omega_0 l}{2}}[f_1(rU + l\omega_0) + f_2(rU + l\omega_0)]$$
$$+(1-\delta_{l0})e^{-\frac{\beta\omega_0 l}{2}}[f_1(rU - l\omega_0) + f_2(rU - l\omega_0)]\Big). \tag{37}$$

The current is expressed as

$$j \equiv \frac{I(V)}{dI_0} = \sum_{r=0}^{d-1} Z_r(n)[na_r^- + (1-n)b_r^-], \tag{38}$$

where

$$a_r^- = \mathcal{Z}\sum_{l=0}^{\infty} I_l\left(\xi\right)\Big(e^{\frac{\beta\omega_0 l}{2}}[f_1(rU - l\omega_0) - f_2(rU - l\omega_0)]$$
$$+(1-\delta_{l0})e^{-\frac{\beta\omega_0 l}{2}}[f_1(rU + l\omega_0) - f_2(rU + l\omega_0)]\Big), \tag{39}$$

$$b_r^- = \mathcal{Z}\sum_{l=0}^{\infty} I_l\left(\xi\right)\Big(e^{\frac{\beta\omega_0 l}{2}}[f_1(rU + l\omega_0) - f_2(rU + l\omega_0)]$$
$$(1-\delta_{l0})e^{-\frac{\beta\omega_0 l}{2}}[f_1(rU - l\omega_0) - f_2(rU - l\omega_0)]\Big). \tag{40}$$

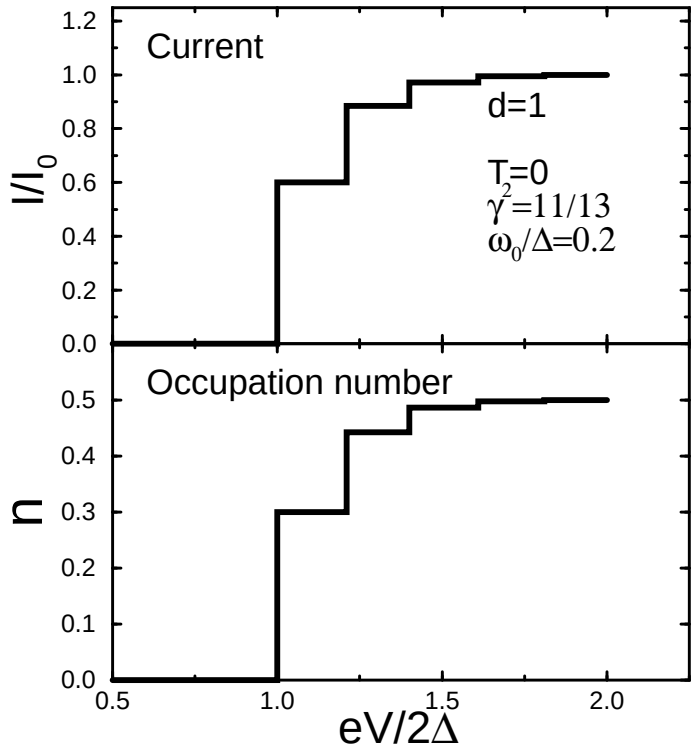


**Fig. 12.** Current-voltage characteristic of the nondegenerate ($d = 1$) MQD at $T = 0$, $\omega_0/\Delta = 0.2$, and $\gamma^2 = 11/13$. There is the phonon ladder in I-V , but no hysteresis.

### 5.4 Absence of switching of single- or double-degenerate MQD

If the transition rates from electrodes to MQD are small, $\Gamma \ll \omega_0$, the rate equation for $n$ and the current, $I(V)$ are readily obtained by using the exact molecular DOS, Eq. (32) and the Fermi-Dirac Golden rule. In particular, for the nondegenerate MQD and $T = 0$K the result is

$$n = \frac{b_0^+}{2 + b_0^+ - a_0^+}, \tag{41}$$

and

$$j = \frac{2b_0^- + a_0^- b_0^+ - a_0^+ b_0^-}{2 + b_0^+ - a_0^+}. \tag{42}$$

The general expressions for the coefficients are given at arbitrary temperatures in Ref.[52], and they are especially simple in low-temperature limit:

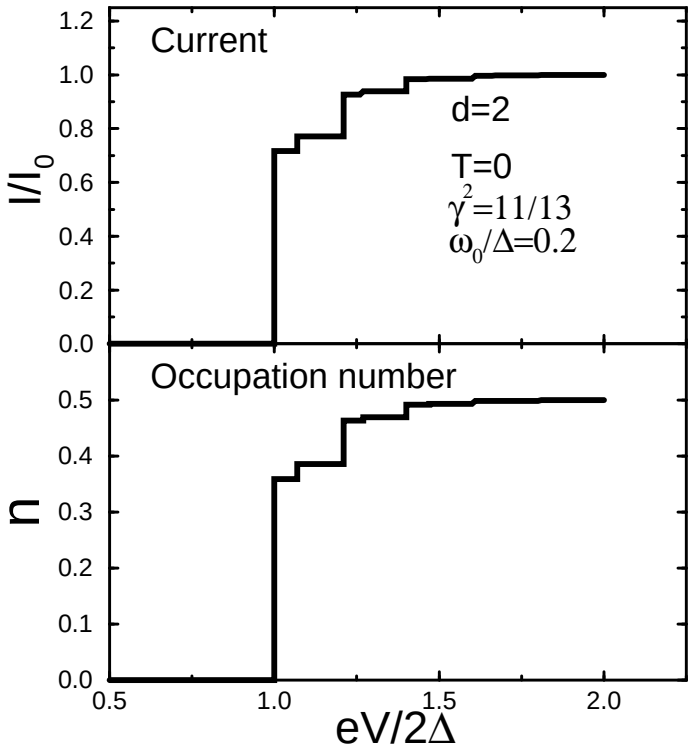


**Fig. 13.** Current-voltage characteristic of two-fold degenerate MQDs ($d = 2$) does not show hysteretic behavior. The parameters are the same as in Fig. 12. Larger number of elementary processes for conductance compared to the nondegenerate case of $d = 1$ generates more steps in the phonon ladder in comparison with Fig. 12.

$$a_0^{\pm} = \mathcal{Z}\sum_{l=0}^{\infty}\frac{|\gamma|^{2l}}{l!}[\theta(l\omega_0 - \Delta + eV/2) \pm \theta(l\omega_0 - \Delta - eV/2)], \tag{43}$$

$$b_0^{\pm} = \mathcal{Z}\sum_{l=0}^{\infty}\frac{|\gamma|^{2l}}{l!}[\theta(-l\omega_0 - \Delta + eV/2) \pm \theta(-l\omega_0 - \Delta - eV/2)], \tag{44}$$

$j = I/I_0$, $I_0 = ed\Gamma$, $\Delta$ is the position of the MQD level with respect to the Fermi level at $V = 0$, and $\theta(x) = 1$ if $x > 0$ and zero otherwise. The current is single valued, Fig. 12, with the familiar steps due to phonon-side bands. The double-degenerate level provides more elementary processes for conductance reflected in larger number of steps on phonon ladder compared to $d = 2$ case, Fig. 13.

On the contrary, the mean-field approximation (MFA) leads to the opposite conclusion. Galperin *et al.* [80] have replaced the occupation number operator $\hat{n}$ in the e-ph interaction by the average population $n_0$ [Eq. (2) of Ref. [80]] and found the average steady-state vibronic displacement $\langle d + d^\dagger \rangle$ proportional to $n_0$ (this is an explicit *neglect* of all quantum fluctuations on the dot accounted for in the exact solution). Then, replacing the displacement operator $d + d^\dagger$ in the bare Hamiltonian, Eq. (11), by its average, Ref. [80], they obtained a new molecular level, $\tilde{\varepsilon}_0 = \varepsilon_0 - 2\varepsilon_{reorg} n_0$ shifted linearly with the average population of the level. This is in stark disagreement with the conventional constant polaronic level shift, Eq. (12,24) ($\varepsilon_{reorg}$ is $|\gamma|^2\omega_0$ in our notations). The MFA spectral function turned out to be highly nonlinear as a function of the population, e.g. for the weak-coupling with the leads $\rho(\omega) = \delta(\omega - \varepsilon_0 - 2\varepsilon_{reorg} n_0)$, see Eq. (17) in Ref. [80]. As a result, the authors of Ref.[80] have found multiple solutions for the steady-state population, Eq. (15) and Fig. 1, and switching, Fig. 4 of Ref. [80], which actually do not exist being an artefact of the model.

In the case of a double-degenerate MQD, $d = 2$, there are two terms, which contribute to the sum over $r$, with $C_0(n) = 1 - n$ and $C_1(n) = n$. The rate equation becomes a quadratic one [52]. Nevertheless there is only one physical root for any temperature and voltage, and the current is also single-valued, Fig. 3.

Note that the mean-field solution by Galperin *et al.* [80] applies at any ratio $\Gamma/\omega_0$, including the limit of interest to us, $\Gamma \ll \omega_0$. where their transition between the states with $n_0 = 0$ and 1 only sharpens, but none of the results change. Therefore, MFA predicts a current bistability in the system where it does not exist at $d = 1$. Ref. [80] plots the results for $\Gamma \geq \omega_0$, $\Gamma \approx 0.1 - 0.3$ eV, which corresponds to molecular bridges with a resistance of about a few 100 k$\Omega$. Such model "molecules" are rather "metallic" in their conductance and could hardly show any bistability at all because carriers do not have time to interact with vibrons on the molecule. Indeed, taking into account the coupling with the leads beyond the second order and the coupling between the molecular and bath phonons could hardly provide any non-linearity because these couplings do not depend on the electron population. This rather obvious conclusion for molecules strongly coupled to the electrodes can be reached in many ways, see e.g. a derivation in Refs. [84, 85]. While Refs. [84, 85] do talk about telegraph current noise in the model, there is no hysteresis in the adiabatic regime, $\Gamma \gg \omega_0$ either. This result certainly has nothing to do with our mechanism of switching [52] that applies to molecular quantum dots ($\Gamma \ll \omega_0$) with $d > 2$. Such regime has not been studied in Refs. [84, 85, 86], which have applied the adiabatic approximation, as being "too challenging problem". Nevertheless, Mitra *et al.* [86] have misrepresented our formalism [52] claiming that it "lacks of renormanlization of the dot-lead coupling" (due to electron-vibron interaction), or "treats it in an average manner". In fact, the formalism [52] is exact, fully taking into account the polaronic renor-

malization, phonon-side bands and polaron-polaron correlations in the exact molecular DOS, Eq. (32).

As a matter of fact, most of the molecules are very resistive, so the actual molecular quantum dots are in the regime we study, see Ref.[87]. For example, the resistance of fully conjugated three-phenyl ring Tour-Reed molecules chemically bonded to metallic Au electrodes [33] exceeds $1\mathrm{G}\Omega$. Therefore, most of the molecules of interest to us are in the regime that we discussed, not that of Refs.[84, 85].

### 5.5 Nonlinear rate equation and switching

Now, consider the case $d = 4$, where the rate equation is non-linear, to see if it produces multiple physical solutions. For instance, in the limit $|\gamma| \ll 1$, $T = 0$, where we have $b_r = a_r$, $\mathcal{Z} = 1$, the remaining interaction is $U = U^C < 0$, we recover the negative-$U$ model [78], and the kinetic equation for $d = 4$ is

$$2n = 1 - (1 - n)^3 \tag{45}$$

in the voltage range $\Delta - |U| < eV/2 < \Delta$. This equation has an additional nontrivial physical solution $n = (3-\sqrt{5})/2 = 0.38$. The current is simplified as $I/I_0 = 2n$. The current-voltage characteristics will show a *hysteretic* behavior in this case for $d = 4$. When the voltage increases from zero, 4-fold degenerate MQD remains in a low-current state until the threshold $eV_2/2 = \Delta$ is reached. Remarkably, when the voltage *decreases* from the value above the threshold $V_2$, the molecule remains in the high-current state down to the voltage $eV_1/2 = \Delta - |U|$ well below the threshold $V_2$.

In fact, there is a hysteresis of current at all values of the electron-phonon constant $\gamma$, e.g. $\gamma^2 = 11/13$ (selected in order to avoid an accidental commensurability of $\omega_0$ and $U$), Fig. 14. Indeed, the exact equation for average occupation of the dot reads

$$\begin{aligned} 2n = {} & (1-n)^3[na_0^+ + (1-n)b_0^+] \\ & +3n(1-n)^2[na_1^+ + (1-n)b_1^+] \\ & +3n^2(1-n)[na_2^+ + (1-n)b_2^+] \\ & +n^3[na_3^+ + (1-n)b_3^+]. \end{aligned} \tag{46}$$

We solved this nonlinear equation for the case $\omega_0/\Delta = 0.2$, $U^C = 0$, so that the attraction between electrons is $U = -2\gamma^2\omega_0 = -0.4$ (all energies are in units of $\Delta$), and found an additional stable solution for an average occupation number (and current) that results in a hysteresis curve, Fig. 14. The bistability region shrinks down with temperature, and the hysteresis loop practically closes at $T/\Delta = 0.01$. As we see from Eqs. (36),(37), the electron levels with phonon sidebands $\Delta \pm l\omega_0$, $\Delta + U \pm l\omega_0$, $\Delta + 2U \pm l\omega_0$, $\Delta + 3U \pm l\omega_0$ with $l = 0, 1, ...$ contribute to electron transport with different weights, and this creates a complex picture of steps on the I-V curve, Fig. 14.

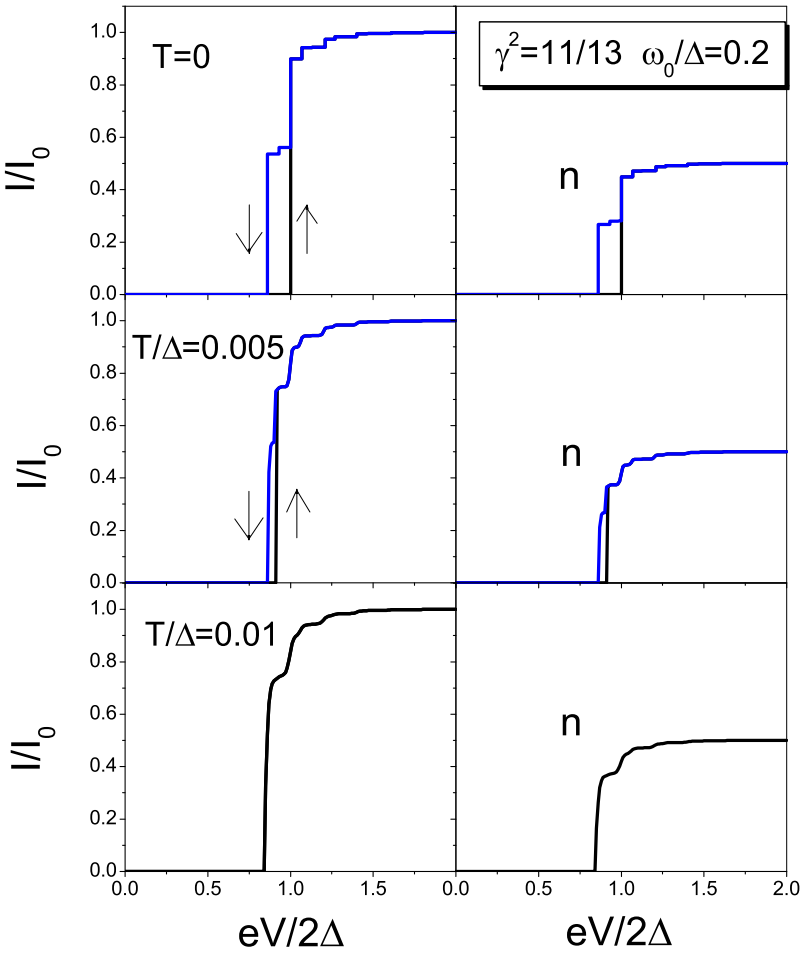


**Fig. 14.** The I-V curves for tunneling through the molecular quantum dot, Fig. 10b with the electron-vibron coupling constant $\gamma^2 = 11/13$.

Note that switching required a degenerate MQD ($d > 2$) and the weak coupling to the electrodes, $\Gamma \ll \omega_0$. Different from the non-degenerate dot, the rate equation for a multi-degenerate dot, $d > 2$, weakly coupled to the leads has multiple physical roots in a certain voltage range and a hysteretic behavior due to *correlations* between different electronic states of MQD [52].

Summarizing this Section, we have calculated the I-V characteristics of the nondegenerate and two-fold degenerate MQDs showing no hysteretic behavior, and conclude that mean field approximation [80] leads to a non-existent hysteresis in a model that was solved exactly in Ref. [52]. Different from the non-degenerate and two-fold degenerate dots, the rate equation for a multi-degenerate dot, $d > 2$, weakly coupled to the leads, has multiple physical roots in a certain voltage range showing hysteretic behavior due to *correlations* between different electronic states of MQD [52]. Our conclusions are important for searching of the current-controlled polaronic molecular switches. Incidentally, $C_{60}$ molecules have the degeneracy $d = 6$ of the lowest unoccupied level, which makes them one of the most promising candidate systems, if the weak-coupling with leads is secured.

## 6 Role of defects in molecular transport

Interesting behavior of electron transport in molecular systems, as described above, refers to ideal systems without imperfection in ordering and composition. In reality, one expects that there will be a considerable disorder and defects in organic molecular films. As mentioned above, the conduction through absorbed [54] and Langmuir-Blodgett [55] monolayers of fatty acids $(CH_2)_n$ was associated with *defects*. An absence of tunneling through self-assembled monolayers of C12-C18 (inferred from an absence of thickness dependence at room temperature) has been reported by Boulas et al. [53]. On the other hand, the tunneling in alkanethiol SAMs was reported in [88, 89], with an exponential dependence of monolayer resistance on the chain length $L$, $R_\sigma \propto \exp(\beta_\sigma L)$, and no temperature dependence of the conductance in C8-C16 molecules was observed over the temperatures $T = 80 - 300$K [89].

The electrons in alkane molecules are tightly bound to the C atoms by $\sigma-$bonds, and the band gap (between the highest occupied molecular orbital, HOMO, and lowest unoccupied molecular orbital, LUMO) is large, $\sim 9-10$eV [53]. In conjugated systems with $\pi-$electrons the molecular orbitals are extended, and the HOMO-LUMO gap is correspondingly smaller, as in e.g. polythiophenes, where the resistance was also found to scale exponentially with the length of the chain, $R_\pi \propto \exp(\beta_\pi L)$, with $\beta_\pi = 0.35\mathring{A}^{-1}$ instead of $\beta_\sigma = 1.08\mathring{A}^{-1}$[88]. In stark contrast with the temperature-independent tunneling results for SAMs [89], recent extensive studies of electron transport through 2.8 nm thick eicosanoic acid (C20) LB monolayers at temperatures 2K-300K have established that the current is practically temperature inde-

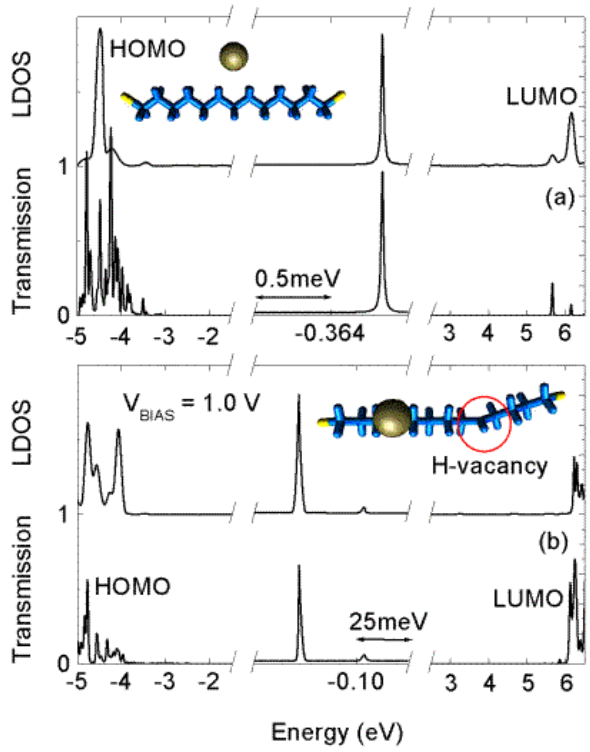


**Fig. 15.** Local density of states and transmission as a function of energy for (a) C13 with Au impurity and (b) C13 with Au impurity and H vacancy (dangling bond). Middle sections show closeups of the resonant peaks due to deep defect levels with respect to the HOMO and LUMO molecular states. The HOMO-LUMO gap is about 10 eV.

pendent below $T < 60$K, but very strongly temperature dependent at higher temperatures $T = 60 - 300$K[90].

A large amount of effort went into characterizing the organic thin films and possible defects there [18, 91, 92]. It has been found that the electrode material, like gold, gets into the body of the film, leading to the possibility of metal ions existing in the film as single impurities and clusters. Electronic states on these impurity ions are available for the resonant tunneling of carriers in very thin films (or hopping in thicker films, a crossover between the regimes depending on the thickness). Depending on the density of the impurity states, with increasing film thickness the tunneling will be assisted by impurity "chains", with an increasing number of equidistant impurities [93].

One-impurity channels produce steps on the I-V curve but no temperature dependence, whereas the inelastic tunneling through pairs of impurities at low temperatures defines the temperature dependence of the film conductance, $G(T) \propto T^{4/3}$, and the voltage dependence of current $I(V) \propto V^{7/3}$[94]. This behavior has been predicted theoretically and observed experimentally for tunneling through amorphous Si [95] and $Al_2O_3$[96]. Due to the inevitable disorder in a "soft" matrix, the resonant states on different impurities within a "channel" will be randomly moving in and out of resonance, creating mesoscopic fluctuations of the I-V curve. The tunneling may be accompanied by interaction with vibrons on the molecule, causing step-like features on the I-V curve [77, 52].

During processing, especially top electrode deposition, small clusters of the electrode material may form in the organic film, causing Coulomb blockade, which also can show up as steps on the I-V curve. It has long been known that a strong applied field can cause localized damage to thin films, presumably due to electromigration and the formation of conducting filaments [56]. The damaged area was about 30nm in diameter in 40-160 monolayer thick LB films [56](a) and 5-10$\mu$m in diameter in films 500-5000Å thick, and showed switching behavior under external bias voltage cycling [56](b). As discussed above, recent spatial mapping of a conductance in LB monolayers of fatic acids with the use of conducting AFM has revealed damage areas 30-100nm in diameter, frequently appearing in samples after a "soft" electrical breakdown, which is sometimes accompanied by a strong temperature dependence of the conductance through the film[58].

A crossover from tunneling at low temperatures to an activation-like dependence at higher temperatures is expected for electron transport through organic molecular films. There are recent reports about such a crossover in individual molecules like the 2nm long Tour wire with a small activation energy $E_a \approx 130$meV [97]. Very small activation energies on the order of 10-100 meV have been observed in polythiophene monolayers [98]. Our present results suggest that this may be a result of interplay between the drastic renormalization of the electronic structure of the molecule in contact with electrodes, and disorder in the film (Fig. 16, right inset). We report the ab-initio calculations of point-defect assisted tunneling through alkanedithiols $S(CH_2)_nS$ and thiophene T3 (three rings $SC_4$) self-assembled on gold electrodes. The length of the alkane chain was in the range $n = 9 - 15$.

We have studied single and double defects in the film: (i) single Au impurity, Figs. 10a,11a, (ii) Au impurity and H vacancy (dangling bond) on the chain, Figs. 16b, 15c, (iii) a pair of Au impurities, Fig. 15b, (iv) Au and a "kink" on the chain (one C=C bond instead of a C-C bond). Single defect states result in steps on the associated I-V curve, whereas molecules in the presence of two defects generally exhibit a negative differential resistance (NDR). Both types of behavior are generic and may be relevant to some observed unusual transport characteristics of SAMs and LB films [54, 55, 58, 90, 97, 98]. We have used an ab-initio approach that combines

the Keldysh non-equilibrium Green's function (NEGF) method with self-consistent pseudopotential-based real space density functional theory (DFT) for systems with *open* boundary conditions provided by semi-infinite electrodes under external bias voltage [51, 49]. All present structures have been relaxed with the Gaussian98 code prior to transport calculations[99]. The conductance of the system at a given energy is found from Eq. (8) and the current from Eq. (4).

The equilibrium position of an Au impurity is about 3Å away from the alkane chain, which is a typical Van-der-Waals distance. As the density maps show (Fig. 16), there is an appreciable hybridization between the s- and d-states of Au and the sp- states of the carbohydrate chain. Furthermore, the $Au^+$ ion produces a Coulomb center trapping a 6s electron state at an energy $\epsilon_i = -0.35$eV with respect to the Fermi level, almost in the middle of the HOMO-LUMO $\sim$ 10eV gap in C$n$. The tunneling evanescent resonant state is a superposition of the HOMO and LUMO molecular orbitals. Those orbitals have a very complex spatial structure, reflected in an asymmetric line shape for the transmission. Since the impurity levels are very deep, they may be understood within the model of "short-range impurity potential" [100]. Indeed, the impurity wave function *outside* of the narrow well can be fairly approximated as

$$\varphi(r) = \sqrt{\frac{2\pi}{\kappa}} \frac{e^{-\kappa r}}{r}, \tag{47}$$

where $\kappa$ is the inverse radius of the state, $\hbar^2\kappa^2/2m^* = E_i$, where $E_i = \Delta - \epsilon_i$ is the depth of the impurity level with respect to the LUMO, and $\Delta$=LUMO$-F$ is the distance between the LUMO and the Fermi level $F$ of gold and, consequently, the radius of the impurity state $1/\kappa$ is small. The energy distance $\Delta \approx 4.8$eV in alkane chains $(CH_2)_n$[53] ($\approx$ 5eV from DFT calculations), and $m^* \sim 0.4$ the effective tunneling mass in alkanes[89]. For one impurity in a rectangular tunnel barrier [100] we obtain the Breit-Wigner form of transmission $T(E, V)$, as before, Eq. (5). Using the model with the impurity state wave function (47), we may estimate for an Au impurity in C13 ($L = 10.9$Å) the width $\Gamma_L = \Gamma_R = 1.2 \times 10^{-6}$, which is within an order of magnitude compared with the calculated value $1.85 \times 10^{-5}$eV. The transmission is maximal and equals unity when $E = \epsilon_i$ and $\Gamma_L = \Gamma_R$, which corresponds to a symmetrical position for the impurity with respect to the electrodes.

The electronic structure of the alkane backbone, through which the electron tunnels to an electrode, shows up in the asymmetric lineshape, which is substantially non-Lorentzian, Fig. 15. The current remains small until the bias has aligned the impurity level with the Fermi level of the electrodes, resulting in a step in the current, $I_1 \approx \frac{2q}{\hbar}\Gamma_0 e^{-\kappa L}$ (Fig. 15a). This step can be observed only when the impurity level is not very far from the Fermi level $F$, such that biasing the contact can produce alignment before a breakdown of the device may occur. The most interesting situations that we have found relate to the

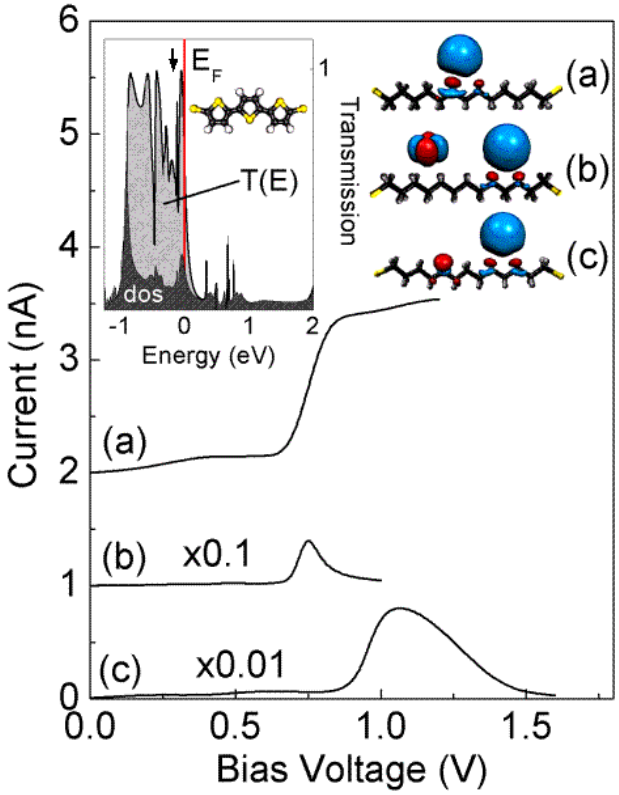


**Fig. 16.** Current-voltage characteristics of an alkane chain C13 with (a) single Au impurity (6s-state), (b) two Au impurities (5d and 6s-states on left and right ions, respectively), and (c) Au impurity and H vacancy (dangling bond). Double defects produce the negative differential resistance peaks (b) and (c). Inset shows the density of states, transmission, and stick model for polythiophene T3. There is significant transmission at the Fermi level, suggesting an ohmic I-V characteristic for T3 connected to gold electrodes. Disorder in the film may localize states close to the Fermi level (schematically marked by arrow), which may assist in hole hopping transport with an apparently very low activation energy (0.01-0.1eV), as is observed.

*pairs* of point defects in the film. If the concentration of defects is $c \ll 1$, the relative number of configurations with pairs of impurities will be very small, $\propto c^2$. However, they give an exponentially larger contribution to the current. Indeed, the optimal position of two impurities is symmetrical, a distance $L/2$ apart, with current $I_2 \propto e^{-\kappa L/2}$. The conductance of a two-impurity chain is [100]

$$g_{12}(E) = \frac{4q^2}{\pi\hbar} \frac{\Gamma_L \Gamma_R t_{12}^2}{|(E-\epsilon_1+i\Gamma_L)(E-\epsilon_2+i\Gamma_R)-t_{12}^2|^2}. \tag{48}$$

For a pair of impurities with slightly differing energies $t_{12} = 2(E_1+E_2)e^{-\kappa r_{12}}/\kappa r_{12}$, where $r_{12}$ is the distance between them. The interpretation of the two-impurity channel conductance (48) is fairly straightforward: if there were no coupling to the electrodes, i.e. $\Gamma_L = \Gamma_R = 0$, the poles of $g_{12}$ would coincide with the bonding and antibonding levels of the two-impurity "molecule". The coupling to the electrodes gives them a finite width and produces, generally, two peaks in conductance, whose relative positions in energy change with the bias. The same consideration is valid for longer chains too, and gives an intuitive picture of the formation of the impurity "band" of states. The maximal conductivity $g_{12} = q^2/\pi\hbar$ occurs when $\epsilon_1 = \epsilon_2$, $\Gamma_L\Gamma_R = t_{12}^2 = \Gamma_2^2$, where $\Gamma_2$ is the width of the two-impurity resonance, and it corresponds to the symmetrical position of the impurities along the normal to the contacts separated by a distance equal to half of the molecule length, $r_{12} = L/2$. The important property of the two-impurity case is that it produces negative differential resistance (NDR). Indeed, under external bias voltage the impurity levels shift as

$$\epsilon_i = \epsilon_{i0} + qVz_i/L, \tag{49}$$

where $z_i$ are the positions of the impurity atoms counted from the center of the molecule. Due to disorder in the film, under bias voltage the levels will be moving in and out of resonance, thus producing NDR peaks on the I-V curve. The most pronounced negative differential resistance is presented by a gold impurity next to a Cn chain with an H-vacancy on one site, Fig. 15b (the defect corresponds to a dangling bond). The defects result in two resonant peaks in transmission. Surprisingly, the H vacancy (dangling bond) has an energy very close to the electrode Fermi level $F$, with $\epsilon_i = -0.1$eV (Fig. 15b, right peak). The relative positions of the resonant peaks move with an external bias and cross at 1.2V, producing a pronounced NDR peak in the I-V curve, Fig. 16c. No NDR peak is seen in the case of an Au impurity and a kink C=C on the chain because the energy of the kink level is far from that of the Au 6s impurity level. The calculated values of the peak current through the molecules were large: $I_p \approx 90$ nA/molecule for an Au impurity with H vacancy, and $\approx 5$ nA/molecule for double Au impurities.

We have observed a new mechanism for the NDR peak in a situation with two Au impurities in the film. Namely, Au ions produce two sets of deep impurity levels in Cn films, one stemming from the 6s orbital, another from the 5d shell, as clearly seen in Fig. 16b (inset). The 5d-states are separated

in energy from 6s, so that now the tunneling through s-d pairs of states is allowed in addition to s-s tunneling. Since the 5d-states are at a lower energy than the s-state, the d- and s-states on different Au ions will be aligned at a certain bias. Due to the different angular character of those orbitals, the tunneling between the s-state on the first impurity and a d-state on another impurity will be described by the hopping integral analogous to the Slater-Koster $sd\sigma$ integral. The peak current in that case is smaller than for the pair Au-H vacancy, where the overlap is of $ss\sigma$ type (cf. Figs. 16b,c).

Thiophene molecules behave very differently since the $\pi-$states there are conjugated and, consequently, the HOMO-LUMO gap is much narrower, just below 2 eV. The tail of the HOMO state in the T3 molecule (with three rings) has a significant presence near the electrode Fermi level, resulting in a practically "metallic" density of states and hence ohmic I-V characteristic. This behavior is quite robust and is in apparent disagreement with experiment, where tunneling has been observed[88]. However, in actual thiophene devices the contact between the molecule and electrodes is obviously very poor, and it may lead to unusual current paths and temperature dependence[98].

We have presented the first parameter-free DFT calculations of a class of organic molecular chains incorporating single or double point defects. The results suggest that the present generic defects produce deep impurity levels in the film and cause a resonant tunneling of electrons through the film, strongly dependent on the type of defects. Thus, a missing hydrogen produces a level (dangling bond) with an energy very close to the Fermi level of the gold electrodes $F$. In the case of a single impurity, it produces steps on the I-V curve when one electrode's Fermi level aligns with the impurity level under a certain bias voltage. The two-defect case is much richer, since in this case we generally see a formation of the negative-differential resistance peaks. We found that the Au atom together with the hydrogen vacancy (dangling bond) produces the most pronounced NDR peak at a bias of 1.2V in C13. Other pairs of defects do not produce such spectacular NDR peaks. A short range impurity potential model reproduces the data very well, although the actual lineshape is different.

There is a remaining question of what may cause the strong temperature dependence of conductance in "simple" organic films like $[CH_2]_n$. The activation-like conductance $\propto \exp(-E_a/T)$ has been reported with a small activation energy $E_a \sim 100 - 200$meV in alkanes [90, 97] and even smaller, 10-100 meV, in polythiophenes [98]. This is much smaller than the value calculated here for alkanes and expected from electrical and optical measurements on $C_n$ molecules, $E_a \sim \Delta \sim 4$eV [53], which correspond nicely to the present results. In conjugated systems, however, there may be rather natural explanation of small activation energies. Indeed, the HOMO in T3 polythiophene on gold is dramatically broadened, shifted to higher energies and has a considerable weight at the Fermi level. The upward shift of the HOMO is just a consequence of the work function difference between gold and the molecule. In the presence of (inevitable) disorder in the film some of the electronic states

on the molecules will be localized in the vicinity of $E_F$. Those states will assist the thermally activated hopping of holes within a range of small activation energies $\leq 0.1$ eV. Similar behavior is expected for Tour wires[97], where $E_F - \text{HOMO} \sim 1$ eV[51](c), if the electrode-molecule contact is poor, as is usually the case.

With regards to carrier hopping in monolayers of saturated molecules, one may reasonably expect that in many studied cases the organic films are riddled with metallic protrusions (filaments), emerging due to electromigration in a very strong electric field, and/or metallic, hydroxyl, etc. inclusions[56, 58]. It may result in a much smaller tunneling distance $d$ for the carriers and the image charge lowering of the barrier. The image charge lowering of the barrier in a gap of width $d$ is $\Delta U = q^2 \ln 4/(\epsilon d)$, meaning that a decrease of about 3.5eV may only happen in an unrealistically narrow gap $d = 2 - 3$Å in a film with dielectric constant $\epsilon = 2.5$, but it will add to the barrier lowering. More detailed characterization and theoretical studies along these lines may help to resolve this very unusual behavior. We note that such a mechanism cannot explain the crossover with temperature from tunneling to hopping reported for single molecular measurements, which has to be a property of the device, but not a single molecule [97].

## 7 Conclusions

Studying molecules as possible building blocks for ultradense electronic circuits is a fascinating quest that spans of over 30 years. It was inspired decades ago by the notion that silicon technology is approaching its limiting feature size, estimated at around 1985 to be about 1$\mu$m[101]. More than thirty years later and with FET gate lengths getting below 10nm [102], the same notion that silicon needs to be replaced at some point by other technologies floats again. We do not know whether alternatives will continue to be steamrollered by silicon technology, which is a leading nanotechnology at the moment, but the mounting resistance to the famed Moore's law requires to look hard at other solutions for power dissipation, leakage current, crosstalk, speed, and other very serious problems. There are very interesting developments in studying electronic transport through molecular films but the mechanisms of some observed conductance "switching" and/or nonlinear electric behavior remain elusive, and this interesting behavior remains intermittent and not very reproducible. Most of the currently observed switching is extrinsic in nature. For instance, we have discussed the effect of molecule-electrode contact: the tilting of the angle at which the conjugated molecule attaches to the electrode may dramatically change its conductance, and that probably explains extrinsic "telegraph" switching observed in Tour wires [23, 34] and molecule reconfigurations may lead to similar phenomena in other systems[67]. Defects in molecular films have also been discussed and may result in spurious peaks in I-V curves. We have outlined some designs of the molecules that may demon-

strate rectifying behavior, which we call molecular "quantum dots". We have shown that at least in some special cases molecular quantum dots may exhibit fast (∼THz) intrinsic switching.

The author is grateful to Jeanie Lau, Jason Pitters and Robert Wolkow for kind permission to use their data and figures. The work has been partly supported by DARPA.

## References

1. J.M. Tour, Acc. Chem. Res. **33**, 791 (2000).
2. C. Joachim, Nanotechnology **13**, R1 (2002).
3. A. Aviram and M.A. Ratner, Chem. Phys. Lett. **29**, 277 (1974).
4. A.S. Martin, J.R. Sambles, and G.J. Ashwell, Phys. Rev. Lett. **70**, 218 (1993); R. M. Metzger, B. Chen, U. Höpfner, M. V. Lakshmikantham, D. Vuillaume, T. Kawai, X. Wu, H. Tachibana, T. V. Hughes, H.Sakurai, J. W. Baldwin, C. Hosh, M. P. Cava, L. Brehmer, and C. J. Ashwell, J. Am. Chem. Soc. **119**, 10455 (1997).
5. K. Stokbro, J. Taylor, and M. Brandbyge, J. Am. Chem. Soc. **125**, 3674 (2003).
6. J.C. Ellenbogen and J. Love, IEEE Proc. **70**, 218 (1993).
7. A.S. Davydov, *Theory of Molecular Excitons* (McGraw-Hill, New York, 1962).
8. F. Gutmann, Nature **219**, 1359 (1968).
9. A.S. Davydov, J. Theor. Biol. **66**, 379 (1977); A.S. Davydov and N.I. Kislukha, Phys. Status Solidi (b) **75**, 735 (1976).
10. A. Scott, Phys. Reports **217**, 1 (1992).
11. J.F. Scott, *Ferroelectric Memories* (Springer, Berlin, 2000).
12. G. Atwood and R. Bez, presentation at ISIF11 (Honolulu, 21-27 April, 2006); W.Y. Cho et al., ISSCC Dig. Tech. papers (2004); G. Wicker, SPIE **3891**, 2 (1999); S.R. Ovshinsky, Phys. Rev. Lett. **21**, 1450 (1968).
13. D. J. Jung, K. Kim, and J. F. Scott, J. Phys. Condens. Mat.**17**, 4843 (2005).
14. Y. Hiranaga and Y. Cho, 11th Intl. Mtg. Ferroel. (IMF 11, Iguassu Falls, Brazil, Sep 5-9, 2005).
15. T. I. Kamins, Interface **14**, 46 (2005); Self-assembled semiconductor nanowires, in *The Nano-Micro Interface*, edited by H. J. Fecht and M. Werner (Wiley-VCH, 2004), p. 195.
16. E. Rabani, D.R. Reichman, P.L. Geissler, and L.E. Brus, Nature **426**, 271 (2003).
17. M.C. Petty, *Langmuir-Blodgett Films* (Cambridge University Press, Cambridge, 1996).
18. A. Ulman, *Characterization of Organic Thin Films* (Butterworth-Heinemann, Boston, 1995).
19. G. Snider, P. Kuekes, and R.S. Williams, Nanotechnology **15**, 881 (2004).
20. B. Stadlober, M. Zirkl, M. Beutl, G. Leising, S. Bauer-Gogonea, and S. Bauer, Appl. Phys. Lett. **86**, 242902 (2005); J.M. Shaw and P.F. Seidler, IBM J. Res. Dev. **45**, 3 (2001).
21. S. Datta *et al.*, Phys. Rev. Lett. **79**, 2530 (1997).
22. A.M. Bratkovsky and P.E. Kornilovitch, Phys. Rev. B **67**, 115307 (2003).
23. P.E. Kornilovitch and A.M. Bratkovsky, Phys. Rev. B **64**, 195413 (2001).

24. N. Ness, S. A. Shevlin, and A. J. Fisher, Phys. Rev. B **63**, 125422 (2001).
25. W.P. Su and J.R. Schrieffer, Proc. Natl. Acad. Sci. **77**, 5626 (1980); S.A. Brazovskii, Sov. Phys. - JETP **51**, 342 (1980).
26. S. A. Brazovskii and N. N. Kirova, Zh. Eksp. Teor. Fiz. Pis'ma Red. **33**, 6 (1981) [JETP Lett. **33**, 4 (1981)].
27. A. Feldblum *et al.*, Phys. Rev. B **26**, 815 (1982).
28. R.R. Chance, J.L. Bredas, and R. Silbey, Phys. Rev. B **29**, 4491 (1984).
29. M.G. Ramsey *et al.*, Phys. Rev. B **42**, 5902 (1990).
30. D. Steinmuller, M.G. Ramsey, and F.P. Netzer, Phys. Rev. B **47**, 13323 (1993).
31. L.S. Swanson *et al.*, Synth. Metals **55**, 241 (1993).
32. M. Jaiswal and R. Menon, Polymer Intl. 55, 1371 (2006).
33. J. Chen, M. A. Reed, A. M. Rawlett, and J. M. Tour, Science **286**, 1550 (1999).
34. Z.J. Donhauser, B.A. Mantooth, K.F. Kelly, L.A. Bumm, J.D. Monnell, J.J. Stapleton, D.W. Price, Jr., A. M. Rawlett, D. L. Allara, J. M. Tour, and P. S. Weiss, Science **292,** 2303 (2001); Z. J. Donhauser, B.A. Mantooth, T.P. Pearl, K.F. Kelly, S.U. Nanayakkara, and P.S. Weiss, Jpn. J. Appl. Phys. **41**, 4871 (2002).
35. C. Li, D. Zhang, X. Liu, S. Han, T. Tang, C. Zhou, W. Fan, J. Koehne, J. Han, M. Meyyappan, A.M. Rawlett, D.W. Price, and J.M. Tour, Appl. Phys. Lett. **82**, 645 (2003); M.A. Reed, J. Chen, A.M. Rawlett, D.W. Price, and J. M. Tour, Appl. Phys. Lett. **78**, 3735 (2001).
36. C.P. Collier, E. W. Wong, M. Belohradský, F. M. Raymo, J. F. Stoddart, P. J. Kuekes, R. S. Williams, and J. R. Heath, Science **285**, 391 (1999); C.P. Collier, G. Mattersteig; E.W. Wong, Y. Luo, K. Beverly, J. Sampaio, F.M. Raymo, J.F. Stoddart, J.R. Heath, Science **289**, 1172 (2000).
37. Y. Chen, D.A.A. Ohlberg, X. Li, D.R. Stewart, and R.S. Williams, J.O. Jeppesen, K.A. Nielsen, and J.F. Stoddart, D.L. Olynick, and E. Anderson, Appl. Phys. Lett. **82**, 1610 (2003); Y. Chen, G.Y. Jung, D.A A Ohlberg, X. Li, D.R Stewart, J.O Jeppesen, K.A Nielsen, J F. Stoddart, and R S. Williams, Nanotechnology **14** 462 (2003).
38. D. R. Stewart, D. A. A. Ohlberg, P. A. Beck, Y. Chen, R. S. Williams, J. O. Jeppesen, K. A. Nielsen, and J. F. Stoddart, Nanoletters **4**, 133 (2004).
39. *Molecular Switches*, edited by Ben L. Feringa (Wiley-VCH, 2001).
40. G. Zheng, F. Patolsky, Yi Cui, W.U. Wang, C.M. Lieber, Nature Biotechnology **23**, 1294 (2005).
41. A. Bachtold, P. Hadley, T. Nakanishi, and C. Dekker, Science **294**: 1317 (2001); P.G. Collins, M.S. Arnold, and P.Avouris, Science **292**, 706 (2001); T. Rueckes, K. Kim, E. Joselevich, G.Y. Tseng, C.-L. Cheung, and C.M. Lieber, Science **289**, 94 (2000).
42. M. Ouyang and D.D. Awschalom, Science **301**, 1074 (2003).
43. C. Krzeminski, C. Delerue, G. Allan, D. Vuillaume, and R.M. Metzger, Phys. Rev. B **64**, 085405 (2001).
44. C. Zhou, M.R. Deshpande, M.A. Reed, L. Jones II, and J.M. Tour, Appl. Phys. Lett. **71**, 611 (1997).
45. Y. Xue, S.Datta, S. Hong, R. Reifenberger, J.I. Henderson, C.P. Kubiak, Phys. Rev. B **59**, 7852(R) (1999).
46. J. Reichert, R. Ochs, D. Beckmann, H. B. Weber, M. Mayor, and H. v. Löhneysen, Phys. Rev. Lett. **88**, 176804 (2002).
47. P.E. Kornilovitch, A.M. Bratkovsky, and R.S. Williams, Phys. Rev. B **66**, 165436 (2002).

48. S. Lenfant, C. Krzeminski,C. Delerue, G. Allan, D. Vuillaume, Nanoletters **3**, 741 (2003).
49. B. Larade and A.M. Bratkovsky, Phys. Rev. B **68**, 235305 (2003).
50. S. Chang, Z. Li, C.N. Lau, B. Larade, and R.S. Williams, Appl. Phys. Lett. **83**, 3198 (2003).
51. J. Taylor, H. Guo and J. Wang, Phys. Rev. B **63**, R121104 (2001); *ibid.* **63**, 245407 (2001); A.P. Jauho, N.S. Wingreen and Y. Meir, Phys. Rev. B **50**, 5528 (1994).
52. A.S. Alexandrov and A.M. Bratkovsky, Phys. Rev. B **67**, 235312 (2003).
53. C. Boulas, J.V. Davidovits, F. Rondelez, and D. Vuillaume, Phys. Rev. Lett. **76**, 4797 (1996).
54. E.E. Polymeropoulos and J. Sagiv, J. Chem. Phys. **69**, 1836 (1978).
55. R.H. Tredgold and C.S. Winter, J. Phys. D **14**, L185 (1981).
56. H. Carchano, R. Lacoste, and Y. Segui, Appl. Phys. Lett. **19**, 414 (1971); N.R. Couch, B. Movaghar, and I.R. Girling, Sol. St. Commun. **59**, 7 (1986).
57. I. Shlimak and V. Martchenkov, Sol. State Commun. **107**, 443 (1998).
58. C.N. Lau, D. Stewart, R.S. Williams, and D. Bockrath, Nano Lett. **4**, 569 (2004).
59. J. Rodriguez Contreras, H. Kohlstedt, U. Poppe, R. Waser, C. Buchal, and N. A. Pertsev, Appl. Phys. Lett. **83**, 4595 (2003).
60. R.A. Wassel, G.M. Credo, R.R. Fuierer, D.L. Feldheim, C.B. Gorman, J. Am. Chem. Soc. **126**, 295 (2004).
61. J. He and S.M. Lindsay, J. Am. Chem. Soc. **127**, 11932 (2005).
62. J. Gaudioso, L.J. Lauhon, and W. Ho, Phys. Rev. Lett. **85**, 1918 (2000).
63. S.-W. Hla, G. Meryer, and K.-H. Rieder, Chem. Phys. Lett. **370**, 431 (2003).
64. G. Yang and G. Liu, J. Phys. Chem. B **107**, 8746 (2003).
65. A. Salomon, R. Arad-Yellin, A. Shanzer, A. Karton, and D.J. Cahen, Am. Chem. Soc. **126**, 11648 (2004).
66. N.P. Guisinger, M.E. Greene, R. Basu, A.S. Baluch, M.C. Hersam, Nano Lett. **4**, 55 (2004).
67. J.L. Pitters and R.A. Wolkow, Nano Lett. **6**, 390 (2006).
68. T. Rakshit, G.C. Liang, A.W. Ghosh, and S. Datta, Nano Lett. **4**, 1803 (2004).
69. A.V. Bune, V.M. Fridkin, S. Ducharme, L.M. Blinov, S.P. Palto, A. Sorokin, S.G. Yudin, and A. Zlatkin, Nature **391**, 874 (1998).
70. S. Ducharme, V. M. Fridkin, A. V. Bune, S. P. Palto, L. M. Blinov, N. N. Petukhova, and S. G. Yudin, Phys. Rev. Lett. **84**, 175 (2000).
71. A.M. Bratkovsky and A.P. Levanyuk, Phys. Rev. Lett. **87**, 019701 (2001).
72. A. Bune, S. Ducharme, V. Fridkin, L.Blinov, S. Palto, N. Petukhova, and S. Yudin, Appl. Phys. Lett. **67** 3975 (1995).
73. T. Furukawa, M. Date, M. Ohuchi, and A. Chiba, J. Appl. Phys. **56**, 1481 (1984).
74. P.E. Kornilovitch, A.M. Bratkovsky, and R.S. Williams, Phys. Rev. B **66**, 245413 (2002).
75. D.V. Averin and K.K. Likharev, in: *Mesocopic Phenomena in Solids*, edited by B.L. Altshuler *et al.* (North-Holland, Amsterdam, 1991).
76. H. Park, J. Park, A.K.L. Lim, E.H. Anderson, A.P. Alivisatos, and P.L. McEuen, Nature **407**, 57 (2000); J. Park, A.N. Pasupathy, J.I. Goldsmith, C. Chang, Y. Yaish, J.R. Petta, M. Rinkoski, J.P. Sethna, H.D. Abruña, P.L. McEuen, and D.C. Ralph, *ibid.* **417,** 722 (2002); W. Liang, M.P. Shores, M. Bockrath, J.R. Long, and H. Park, *ibid.* **417**, 725 (2002).

77. N.B. Zhitenev, H. Meng, and Z. Bao, Phys. Rev. Lett. **88**, 226801 (2002).
78. A.S. Alexandrov, A.M. Bratkovsky, and R.S. Williams, Phys. Rev. B **67**, 075301 (2003).
79. A.S. Alexandrov and A.M. Bratkovsky, cond-mat/0606366.
80. M. Galperin, M.A. Ratner, and A. Nitzan, Nano Lett. **5**, 125 (2005).
81. A.S. Alexandrov and N.F. Mott, *Polarons and Bipolarons* (World Scientific, Singapore, 1996).
82. Y. Meir and N.S. Wingreen, Phys. Rev. Lett. **68**, 2512 (1992).
83. G.D. Mahan, *Many-Particle Physics*, 2nd ed. (Plenum, New York, 1993).
84. A. Mitra, I. Aleiner, and A. Millis, Phys. Rev. Lett. **94**, 076404 (2006).
85. D. Mozyrsky, M. B. Hastings, and I. Martin, Phys. Rev. B **73**, 035104 (2006).
86. A. Mitra, I. Aleiner, and A. Millis, Phys. Rev. B **69**, 245302 (2004).
87. H. Park, J. Park, A.K.L. Lim, E.H. Anderson, A.P. Alivisatos, and P.L. McEuen, Nature **407**, 57 (2000); J. Park, A.N. Pasupathy, J.I. Goldsmith, C. Chang, Y.Yaish, J.R. Retta, M. Rinkoski, J.P. Sethna, H.D. Abruna, P.L. McEuen, and D.C. Ralph, Nature (London) **417**, 722 (2000); W. Liang *et al.*, Nature (London) **417**, 725 (2002).
88. H. Sakaguchi, A. Hirai, F. Iwata, A. Sasaki, and T. Nagamura, Appl. Phys. Lett. **79**, 3708 (2001); X.D. Cui, X. Zarate, J. Tomfohr, O.F. Sankey, A. Primak, A.L. Moore, T.A. Moore, D. Gust, G. Harris, and S. M. Lindsay, Nanotechnology **13**, 5 (2002).
89. W. Wang, T. Lee, and M.A. Reed, Phys. Rev. B **68**, 035416 (2003).
90. D.R. Stewart, D.A.A. Ohlberg, P.A. Beck, C.N. Lau, and R.S. Williams, Appl. Phys. A **80**, 1379 (2005).
91. G.L. Fisher, A.E. Hooper, R.L. Opila, D.L. Allara, and N. Winograd, J. Phys. Chem. B **104**, 3267 (2000); K. Seshadri, A.M. Wilson, A. Guiseppi-Elie, D.L. Allara, Langmuir **15**, 742 (1999).
92. A.V. Walker, T.B. Tighe, O. Cabarcos, M.D. Reinard, S. Uppili, B.C. Haynie, N. Winograd, and D. L. Allara, J. Am. Chem. Soc. **126**, 3954 (2004).
93. M. Pollak and J.J. Hauser, Phys. Rev. Lett. **31**, 1304 (1973); I.M. Lifshitz and V.Ya. Kirpichenkov, Zh. Eksp. Teor. Fiz. **77**, 989 (1979).
94. L.I. Glazman and K.A. Matveev, Sov. Phys. JETP **67**, 1276 (1988).
95. Y. Xu, D. Ephron, and M.R. Beasley, Phys. Rev. B **52**, 2843 (1995).
96. C.H. Shang, J. Nowak, R. Jansen, and J.S. Moodera, Phys. Rev. B **58**, 2917 (1998).
97. Y. Selzer, M.A. Cabassi, T.S. Mayer, D.L.Allara, J. Am. Chem. Soc. **126**, 4052 (2004).
98. N.B. Zhitenev, A. Erbe, and Z. Bao, Phys. Rev. Lett. **92**, 186805 (2004).
99. M. J. Frisch, GAUSSIAN98, Revision A.9, Gaussian, Inc., Pittsburgh, PA, 1998.
100. A.I. Larkin and K.A. Matveev, Zh. Eksp. Teor. Fiz. **93**, 1030 (1987).
101. N.G. Rambidi and V.M.Zamalin, *Molecular Microelectronics: Origin and Outlook* (Znanie, Moscow, 1985).
102. M. Ieong, B. Doris, J. Kedzierski, K. Rim, M.Yang, Science **306**, 2057 (2004).